1 General Introduction

1.1 Foreword

Over the past century, our fundamental understanding of the static atomic-scale structure of matter has been dramatically advanced by direct structural measurements of periodic materials using x-rays. These measurements have progressed from von Laue's discovery of the diffraction of x-rays by crystals in 1912 [1, 2] to the Braggs' initial development of x-ray crystallography in 1913 [3, 4], to Watson and Crick's solution using Rosalind Franklin's x-ray crystallographic data of the structure of DNA in 1953 [5], to Rossman's solution using a synchrotron x-ray source of the structure of the human rhinovirus in 1985 [6], to the very recent demonstration at the LCLS facility of macromolecular structure determination using crystals less than a micron across in 2011 [7].

Due in large part to the capabilities of modern synchrotron-based x-ray facilities, researchers now have access to direct structural probes capable of characterizing a wide variety of systems on atomic length scales. Undulators on modern third-generation storage rings, such as ESRF, APS, and SPring-8, have enabled researchers to push crystallography, diffuse scattering, small-angle scattering, inelastic scattering, and spectroscopic techniques, such as Extended x-ray Absorption Fine Structure (EXAFS) and Near Edge X-ray Absorption Fine Structure (NEXAFS) to highly advanced states. It is now standard practice for geophysicists to study tiny samples under enormous pressures in the small region between the tips of two diamonds, for surface scientists to solve the structure of single ad-layers of atoms on a crystal facet, for materials researchers to monitor the deposition of individual atomic layers, and for biologists to solve the atomic structure of a macromolecule.

Nevertheless, in nature, most materials are neither spatially periodic nor static. Consequently, researchers want to determine the atomic-scale structure of heterogeneous materials as they evolve, react, or carry out their biological function(s). Coherent x-ray beams offer the potential of meeting this challenge. Already, the limited coherence available at modern third-generation storage rings has enabled pioneering efforts to develop techniques such as coherent diffraction imaging (CDI), which take advantage of over-sampling and iterative phase retrieval techniques to eliminate the need for periodic systems. Many of the technologies (Fresnel zone plates, Laue lenses, kinoform lenses) currently being pursued to focus x-ray beams to nanometer focal spots require coherent illumination. Finally, the partial coherence of third-generation sources enabled the development of X-ray Photon Correlation Spectroscopy (XPCS), opening up the study of equilibrium fluctuations of opaque systems and/or at finite-momentum transfer. The pulsed time-structure of storage rings has enabled pioneering efforts in time-resolved x-ray crystallography, diffraction, and x-ray absorption spectroscopies.

Full development of these and other novel techniques requires an x-ray source with orders of magnitude higher coherence at a repetition rate high enough to maintain the time-average flux at the levels of current state-of-the-art facilites. The individual pulses must, however, remain small enough to avoid pushing the peak flux beyond the adiabatic heating limit [8]. In addition, hard x-rays are required for atomic-scale structural measurements. The here described Energy Recovery Linac (ERL) meets all of these challenges.

To understand the relationship between the characteristics of the electron beam and the quality of the radiation produced by an undulator, it is convenient to consider the spectral brightness, $\mathcal{B}$ [9, 10]:

$$\mathcal{B} = \frac{\mathcal{F}}{4\pi^2 \Sigma^T \Sigma^T_{x'} \Sigma^T_y \Sigma^T_{y'}}, \tag{1.1.1}$$

where $\mathcal{F}$ is the spectral flux [photons/s/0.1%BW]; $\Sigma^T_{x,y}$ are the total photon source sizes in the horizontal and vertical directions; and $\Sigma^T_{x',y'}$ are the total photon-beam divergences. High spectral brightness enables the delivery of a very high-flux, monochromatic-photon beam onto a very small sample area with as parallel a beam as possible.

In practice, the spectral brightness of an undulator is determined by the convolution of the radiation produced by a single charged particle passing through the undulator with the phase-space distribution of the particle beam. The phase-space distribution is, in turn, characterized by the emittance, which is the product of the particle-beam size times its angular divergence in orthogonal directions (e.g., horizontal and vertical). Therefore, to maximize the spectral brightness of the x-ray beam, the emittance of the electron beam needs to be minimized. Newer synchrotron-storage-ring sources such as PETRA-III (DESY/Hamburg, Ger.), SLS (Villigen/CH), and soon NSLS-II (Brookhaven/NY), go to great efforts to reduce the electron beam emittance. It is intrinsically difficult to reduce the horizontal electron beam emittance of storage rings, which is far from the ideal. For example PETRA-III has a specified nearly ideal vertical emittance of 10 pm, but a hundred times larger horizontal emittance of 1 nm [11].

There are fundamental limits to how far one can increase the spectral brightness of the photon beam by reducing the emittance of the electron beam. If the emittance of the electron beam is reduced far enough, the intrinsic properties of the radiation field of a single-point charge begin to dominate the source size and divergence. The fundamental limit to the spectral brightness is set by the wave nature of light and occurs when the photon-beam size and divergence are at the diffraction limit. Further reductions in the electron-beam emittance do not increase the spectral brightness of the x-ray beam.

By definition, at the diffraction limit, the x-ray beam has 100% transverse spatial coherence. The coherent fraction is the ratio of the diffraction-limited phase-space $(\lambda/2)^2$ to the actual phase-space of the photon beam. The coherent flux $\mathcal{F}_\mathrm{C}$ is given by [9, 10]

$$\begin{aligned}\mathcal{F}_\mathrm{C} &= \mathcal{B}\left(\frac{\lambda}{2}\right)^2 \\ &= \frac{\mathcal{F}\lambda^2}{16\pi^2 \Sigma^T \Sigma^T_{x'} \Sigma^T_y \Sigma^T_{y'}},\end{aligned} \tag{1.1.2}$$

where λ is the wavelength of the radiation. The λ^2–dependence of the diffraction-limited phase-space is responsible for the challenge in achieving a coherent source of hard x-rays.

Pushing these notions to their fundamental limits, the ultimate synchrotron x-ray source is a high spectral flux, continuous-duty, short pulse (sub-picosecond), coherent (diffraction-limited), hard ($\lambda \leq 1.5$ Å) synchrotron x-ray source. A continuous-duty source (also known as a continuous wave or 'CW' source) is one that delivers x-rays in a continuous train of pulses at rates exceeding a million per second. The parameters of the ERL discussed in this document have tremendous advantages for a wide variety of x-ray experiments.

Imagine for a moment the scientific impact of such an ideal x-ray source. The several orders of magnitude increase in average coherent flux over present-day sources will be of immediate benefit to a large and established synchrotron radiation community. Enhanced transverse coherence is critical for x-ray photon correlation spectroscopy and 3D coherent diffraction imaging. High average brightness at short-pulse length and high-repetition rate will enable unique studies of molecular dynamics using pump and probe diffraction and orientation-sensitive-x-ray spectroscopy. Exceedingly small x-ray-source size and divergence is essential for high-pressure research, materials characterization at sub-micron length scales, and Small Angle X-ray Scattering (SAXS) and Wide Angle X-ray Scattering (WAXS) studies of macromolecule dynamics carried on within micro-fluidic flow cells. The opportunity to fully utilize spectral brightness from a 25 m undulator is unprecedented for applications that demand exceedingly high energy resolution, e.g. inelastic x-ray scattering. Furthermore, the CW Linac of an ERL can also be used to extract ultra-small beam-phase-space volumes that could enable revolutionary new sources like the X-ray Free Electron Laser Oscillator (XFEL-O) [12]. An ERL will enable a broad range of studies that potentially lead to paradigm shifts, resolve long-standing questions, and initiate new fields of investigation in coherent x-ray science.

1.2 Examples of ERL science

What follows is a sampling of experiments especially well suited to an ERL source described in this document. These examples were described in an invited paper [8] that also discussed how the ERL complements X-ray Free Electron Laser (XFEL) sources like the successfully operating LCLS.

1.2.1 What goes on deep inside the earth and planets?

The physics and chemistry of deep earth and planetary materials is one of the most important and least understood areas of science [13, 14]. At 100 to 500 GPa, chemistry is completely altered because the pressure times volume (PV) term in the free energy exceeds the energy of many chemical bonds. Solid-state properties change because outer electron orbitals overlap, leading to altered electrical properties; indeed, at high pressure almost half the periodic table is superconducting. The invention of the Diamond Anvil Cell (DAC) [15] has revolutionized high-pressure science and allowed investigations up to center-of-the-earth pressures of 350 GPa [16]. Often high-pressure samples (see Fig. 1.2.1) are only microns in size; the x-ray beam must penetrate millimeters of diamond and pressurization media, like inert gases, solidify and induce strain in the sample. Sample strains require even smaller probe beams to scan and map strain gradients.

Advantages of an ERL: DAC experiments are severely x-ray-probe-limited, even at the best existing sources. Today a state-of-the-art beamline (APS 16 ID-D) yields 1×10^{10} photons/s/ μm^2 [17]. Focused XFEL nanobeams will be of limited use because the peak intensity will damage diamonds. A focused, monochromatic 30 keV x-ray beam from the 5$^{\text{th}}$

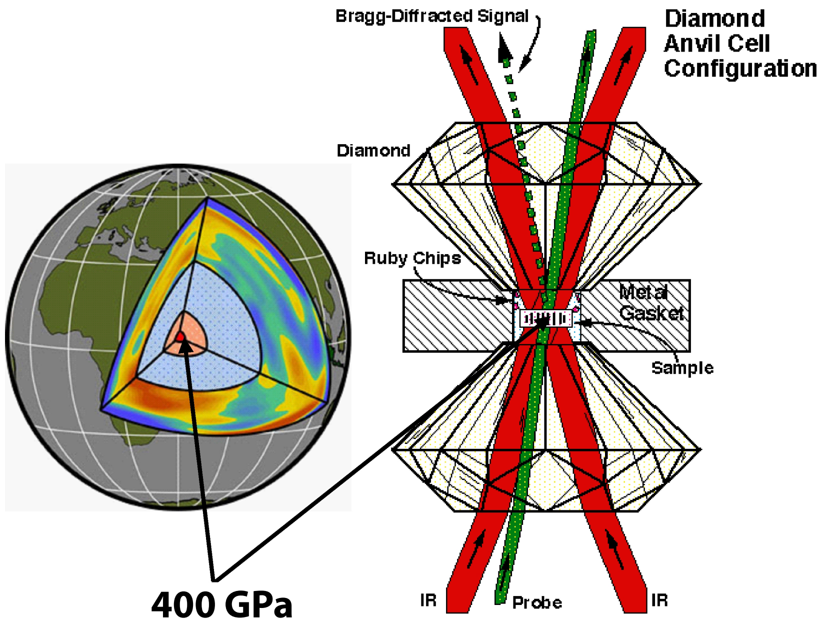

Figure 1.2.1: The Diamond Anvil Cell achieves center-of-the-earth pressures by squeezing specimens between small facets of two gem-quality diamonds.

harmonic of a 5-meter ERL undulator would provide $> 10^{13}$ photons/s/ μm^2. This huge gain will enable presently unfeasible DAC studies that will transform high-pressure research.

For example, little is known about high-dynamical processes that determine phase stability, phase transitions, chemical reactivity, diffusivity, and transport. Numerous chemical reactions occur as heterogeneous earth-forming materials rise through varying conditions of temperature and pressure during volcanic and tectonic events. These reactions affect earthquakes, volcanism, and formation of commercially important mineral deposits. Inside the earth, mixing of chemical species is limited by transport. Because diffusivities vary exponentially with temperature, extrapolating known transport properties to high pressure is prone to large errors and leaves great uncertainties about deep-earth chemistry. Static measurements that are now made at state of the art ring-based hard x-ray sources like the Advanced Photon Sorce (APS) could be made into dynamic measurements at an ERL.

1.2.2 Can we improve polycrystalline materials?

Many materials are polycrystalline and the size, structure, and interfaces between crystalline grains often controls material properties. A detailed understanding of polycrystalline materials, and better methods of synthesis, would have far-reaching and profoundly positive effects on society. One of the grand challenges in materials science is to explain the materials properties of polycrystalline substances starting from the measured properties of large perfect crystals. For instance, crack propagation, fatigue, and failure in the common metals used for bridges and aircraft parts are of great interest.

What has been lacking is sufficiently detailed, 3D, spatially-resolved measurements of de-

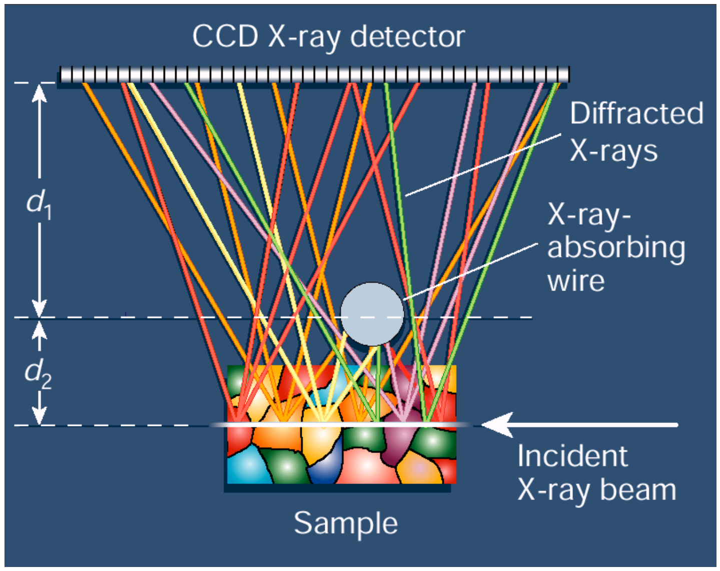

Figure 1.2.2: Differential-Aperture X-Ray Structural Microscopy (DAXM) from UniCAT beamline (APS). Schematic of the focusing geometry and depth profiling technique of DAXM. The x-ray diffraction patterns and analysis provide $\approx 0.01°$ angular resolution used to measure rotation gradients and subgrain structure within crystal grains [19].

formation and microstructure on length scales of a typical grain. Submicron spatial resolution of grains and their interfaces is required to provide definitive benchmarks for theory and simulations. Given such information, scientists could link mesoscopic structure with macroscopic properties to explain strength and failure modes of metals and ceramics, ionic diffusion in fuel cell electrodes, and dynamical properties of alloys. As grains shrink, the relative contribution of the surface to the overall free energy becomes increasingly important. This is why nanocrystalline materials often have very different properties than materials of the same composition with micron-sized grains [18]. Nanocrystalline materials have enormous potential for society, but are even harder to analyze at the single crystal level. Hard x-ray beams are among the few probes that can penetrate and measure polycrystalline grain properties within bulk materials on appropriate length scales. It is necessary to nondestructively study crystal morphology, orientation, strain, texture, and phase with a spatial resolution below the grain size.

Advantages of an ERL: Of particular interest are microstructural studies of crystal grain size and orientation, local elastic strain, and plastic deformation using the Differential Aperture 3D X-ray Microscopy (DAXM) recently developed by the RIS∅ group at the European Synchrotron Radiation Source (ESRF) [20, 21] and by the ORNL group at the APS [22–24]. With DAXM, an x-ray beam focused to submicron size by a pair of crossed Kirkpatrick-Baez mirrors can produce diffraction from crystal grains along the path length in the sample. A series of images are collected as a platinum wire edge is scanned across the sample, shadowing the diffraction pattern and therefore allowing identification of a given Bragg reflection from a diffracting grain at a particular depth, as shown in Fig. 1.2.2. Presently at the APS, a single depth scan requires about 30 minutes and collecting an array of $80 \times 80 \times 80$ voxels takes about

3 hours. With the ERL and appropriate detectors, we estimate that a $1000 \times 1000 \times 1000$ voxel map could be generated in a few seconds, thereby enabling in situ real time experiments, such as rapid annealing, and plastic and elastic deformation [22]. This advance in methodology would have an enormous impact on understanding polycrystalline materials with submicron grains.

Complementary information can be obtained through the use of Coherent Diffraction Imaging (CDI), in which the far-field diffraction pattern (small angle) from a coherently illuminated sample is analyzed to recover the phase of the scattered wave-field. Assuming the structure of the illuminating wavefield is known, this is equivalent to measuring the complex transmission function of the sample. If the sample is a nanocrystal, then each Bragg peak contains a coherent diffraction pattern that can be analyzed to recover a 3D density map of the diffracting crystal, while ignoring neighboring crystals that have different orientations [25]. Bragg coherent diffractive imaging is extremely sensitive to strain; hence, a 3D diffraction pattern about a single Bragg peak can be used to recover a 3D map of the strain projected onto that peak [26]. Researchers at the APS have recently demonstrated the collection of CDI patterns around multiple Bragg peaks of the same crystal, permitting the creation of a 3D map of a 3D strain vector. By taking advantage of the strain sensitivity and orientation selection of Bragg CDI, it should be possible to map in three dimensions the strain due to finite size and boundary effects in an individual grain in a polycrystalline sample, with nanometer resolution.

The application of CDI is limited by the coherent flux that can be delivered to the sample. A 3D coherent diffraction pattern with $\approx 20\,\mathrm{nm}$ resolution currently takes hours to record at the APS. Given the inverse 4th-power relationship between resolution and flux [27] at the proposed ERL a 3D CDI pattern at $\approx 2\,\mathrm{nm}$ from a radiation-hard material could be recorded in a few hours, or a 20 nm resolution pattern recorded in a few seconds. Also, CDI could be performed at considerably higher x-ray energy, in which current beamlines suffer from very short coherence lengths, allowing access to higher order Bragg peaks and permitting the design of experiments using diamond anvil cells.

1.2.3 Can we determine macromolecular structures of molecules that are difficult to crystallize?

Modern bioscience is heavily dependent on the determination of macromolecular structures, the vast majority of which have been determined by x-ray crystallography. Crystallography has been very successful in determining the structure of soluble proteins. Membrane proteins and large protein or protein-nucleic acid complexes constitute a very significant fraction of cellular proteins. Unfortunately, crystallography has been less successful with such samples owing to the difficulty of obtaining suitable crystals. Structure determination by Nuclear Magnetic Resonance (NMR) is limited to relatively small molecules and requires preparation of relatively large amounts of isotopically labeled material. Coherent small-angle electron diffraction can resolve nonperiodic structures with resolution, but the threshold for radiation damage limits the resolution to about 10 Å for biological molecules [28].

An efficient method for solving macromolecular structures to atomic resolution without the need for crystals would certainly be one of the most transformational biological developments in decades. For this reason, a prime motivation for the development of XFELs has been the possibility of determining macromolecular structure from the scattering of individual molecules

[29], thereby foregoing the need to grow crystals. The low XFEL repetition rate, however, will limit the method.

Spence, Chapman, and colleagues have suggested an approach to circumvent the threshold for radiation damage by delivering fresh molecules in a stream of evaporating water droplets. Elliptically polarized laser light would be used to orient a stream of individual molecules [30, 31]. Alternatively, structural information may be obtained from a sufficiently large number of randomly oriented molecules, even when the recorded diffraction is very weak [32].

Another promising approach is to obtain complete data sets by combining data from a large number of randomly oriented, single nanocrystal diffraction patterns. It is widely believed that it is much easier to obtain large quantities of nanocrystals than the few large crystals required for present day analysis at storage-ring sources; indeed, this has been a motivation for recent experiments at the LCLS [7].

Advantages of an ERL: ERLs can achieve greatly increased time-averaged flux density relative to other sources. Calculations on GroEL, a large protein complex, indicate that an ERL beam would allow a 7 Å resolution structure to be obtained in minutes [31], orders of magnitude faster than with alternative sources. The data acquisition time appears to scale as the inverse 4^{th} power of the resolution for this system [31]; therefore ERL sources may be the most practical way to solve many important but difficult-to-crystallize biological structures. Similar arguments apply to diffraction from nanocrystals: While the ERL will not be able to outrace the radiation damage, it will have sufficient intensity to obtain many thousands of nanocrystal diffraction patterns per second. In principle, complete data for complete structures should be obtainable in a very short period of time.

1.2.4 What is the physics of the glass transition?

The 125^{th} anniversary issue of Science magazine identified the glass transition as one of the most important outstanding questions in all of science. Likewise, Nobel laureate Philip Anderson has said that “The deepest and most interesting unsolved problem in solid state theory is probably the nature of glass and the glass transition” [33]. How can it be that a liquid, subject to only short-ranged forces, becomes locked into just one of many possible configurations? Many theoretical and computational models have been offered, but detailed structural information is needed to compare competing approaches with realistic atomic assemblies. It has long been recognized that what is needed are better measurements of correlation functions of materials undergoing the glass transition. Ideally, one would like to determine the 3D position of every atom in a volume of glass prepared under different conditions, i.e., the specific atomic structure of the glass. Since glass lacks translational order, crystallographic methods cannot be used to determine the specific atomic structure of a glass particle.

Advantages of an ERL: This information may be obtainable with an ERL. The highly coherent, high-average flux capabilities of the ERL provide two independent and complimentary approaches to study the glass transition: One approach is to use lensless reconstruction procedures [34, 35] to determine the 3D positions of all atoms in a nanoparticle of glass, such as a metallic glass. The ability to study the atomic structure of amorphous materials would be a true breakthrough for materials sciences and physics. A second approach would measure atomic correlations that give rise to the time-varying speckle patterns analyzed by XPCS [36]. This experiment is ideally suited for the ERL. Factors of 10^2 to 10^3 higher coherent flux enables studies of ergodic processes that probe 10^4 to 10^6 faster time scales or have much larger signal-to-noise ratio than experiments currently under study at existing synchrotrons.

A very recent and exciting demonstration of cross-correlation analysis of the scattering produced by coherent beam illumination has been published [37]. The work shows how a 4-point cross-correlation function can be used to explore local symmetries in colloidal glasses. X-ray scattering from a coherently illuminated disordered (glassy state) liquid produces the usual Q-dependent pattern of radial rings (corresponding to length scales). If however the time scale of structure change is slow compared to measurement time, each ring is a speckle pattern. Analyzing angular correlations within the ring (comparing speckle intensity vs. angle separation around the ring), the authors find hidden azimuthal symmetry (particular n-fold patterns are associated with particular rings). Simulations show this to be consistent with close-packed random ensembles of icosahedral clusters. A specific fascinating result, which the authors call dynamic heterogeneity, was found in a ring at $Q = 0.04$/nm that evolves from 6- to 5-fold symmetry without a measurable intermediary. Similar phenomena are found in molecular dynamics simulations when icosohedral clusters reorganize in different orientations as bonds break and form.

This work has the potential to be extended to solution systems where the characteristic time for structural change is microseconds rather than seconds. It would require collecting statistically meaningful images before the speckles are averaged away by temporal change. To accomplish this, one needs coherent beams of much higher intensity, short x-ray pulses, and new detectors that collect and store images very rapidly or contain on-board electronics to perform the angular correlation following each exposure. An XFEL is an obvious source for such work. However, an ERL has some interesting advantages based on the high time-averaged flux, because one could study one sample through multiple exposures and, therefore, follow the time evolution during non-equilibrium conditioning/processing. It may be possible, for example, to understand the local order just before crystallization. A 10 μm aperture was used to get partial coherence at ESRF ID10A and data were collected by averaging 50 to 100, 0.15 s – 0.4 s images [37]. In order not to smooth out the speckle pattern the total exposure time, several tens of seconds, was matched to the sample relaxation time. At 8 keV, the ERL (hi-coherence mode) will produce radiation with roughly 200 times higher coherent fraction than ESRF, shown in Fig. 1.3.3. The ERL produces a beam with isotropic 2D transverse coherence, so speckle contrast would be of equal quality around the ring. The nominal ERL pulse structure, 2 ps separated by 770 ps, will allow for optimization of exposure by selecting the number of pulses per image. This will enable high precision studies of dynamics (along with spatial and angular correlations) by determining how speckle contrast depends on exposure pulse number.

1.2.5 Can we understand the dynamics of macromolecules in solution?

Many vitally important processes involve changes of macromolecular structure in solution. Changes in solution pH, solvent or ionic environment cause proteins and nucleic acids to fold and unfold, polymers to collapse or disperse, cell cytoskeletal proteins to assemble or disassemble, multimers to come apart or aggregate, macromolecules to adsorb or desorb from surfaces, and motor proteins to change the way they ‘walk’ along tubulin fibers. Understanding these processes experimentally requires a means for rapidly changing solution conditions

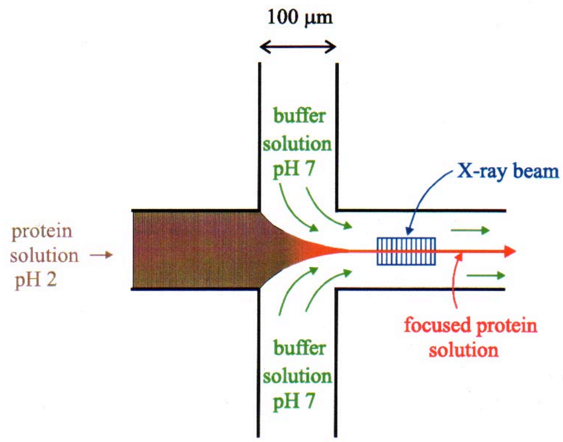

Figure 1.2.3: A micromixer utilizes diffusional equilibrium of the lamellar flow of a submicrometer wide jet between side-streams in a lithographically-fabricated mixer cell. Microsecond mixing times occur with submicron-wide jets.

and a method to probe the subsequent structural alterations. Conventional x-ray methods are limited to changes on millisecond time scales, and even then are feasible only if adequate quantities of solution are available. These limitations exclude the vast majority of macromolecular systems of interest. The recent invention of the lamellar-flow x-ray micromixer [38, 39], shown in Fig. 1.2.3, allows solution conditions to be changed on microsecond time scales. These mixers take advantage of the fact that diffusional equilibrium occurs on microsecond time-scales for adjacent lamellar flows that are submicron in thickness, and require low-volume, micron-wide streams that conserve scarce chemicals. Lamellar micromixers have been applied to understand protein [39, 40] and nucleic acid folding [41, 42] using Small-Angle X-ray Scattering (SAXS).

Advantages of an ERL: Solution SAXS is inherently weak and signal strength is exacerbated by specimen dilution and the very small diffracting volumes inside the mixers central lamellar stream. Experimentally, the signal-to-noise is ultimately set by the strength of scatter from the macromolecule solution relative to that from the illuminated side-streams. This necessitates probe beams that are both intense and of submicron size to interrogate the central stream with minimal inclusion of side-streams. Micromixer experiments are presently limited by source brightness to millisecond or greater time resolution at even the most intense x-ray sources. The extremely intense ERL beams will open a new frontier in studies on protein molecule dynamics not presently accessible, enabling micromixer experiments at microsecond or shorter timescales and studies of more weakly scattering systems while providing higher spatial resolution.

1.2.6 Can we better understand interfacial processes and defects?

Interfaces profoundly influence the behavior of electronic devices and chemical reactions. Yet surface defects are extraordinarily hard to visualize and analyze: they are nonperiodic and occur at very low areal densities. Most often defects disrupt underlying surface periodicity

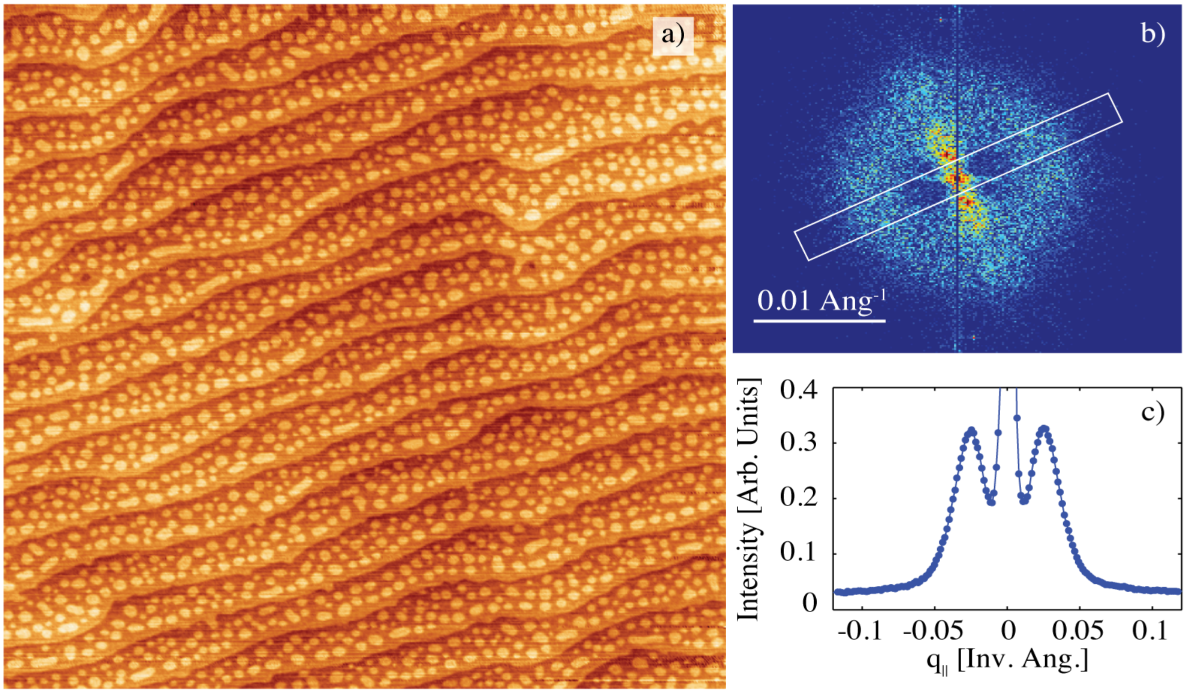

Figure 1.2.4: a) Atomic force microscope image of $< 001 >$ $SrTiO_3$ after pulsed-laser-deposition growth of 11.3 layers of $SrTiO_3$. b) Fourier transformation of the AFM image, illustrating speckle in the diffuse 'Henzler rings' associated with the island structure. c) Diffuse scattering profile corresponding to the rectangular region in b, experimentally measured with an incoherent beam [44].

and have an elemental composition similar (if not equal) to the substrate. In these cases, the defects perturb the electronic structure, but fail to fluoresce at a distinguishable x-ray wavelength. Electron methods (e.g., RHEED, etc.) are of limited use with buried interfaces, or if the environment of interest is not compatible with high vacuum as in a reaction chamber.

Advantages of an ERL: A new phase contrast, full-field imaging technique called x-ray reflection interface microscopy allows visualization of molecular scale features at interfaces and on crystal surfaces [43]. However, the method is currently limited by available total flux, since the reflected intensity is generally at best 10^{-5} lower than the incident intensity, and the condensing and objective zone-plate optics further reduce the available flux by 10^{-2}. Feasibility experiments at the APS with $\approx 10^{12}$ photons/s incident flux required an hour to image a sample. With an ERL beam, the spectral brightness and total available flux would be increased by a factor of 10^4, and would reduce the acquisition time to a fraction of a second. Improvements in integration time for single images could enable studies of nucleation and step movements during *in-situ* growth. With the ERL's high coherent flux, coherence-based contrast mechanisms like ptychography could be explored.

As an example, Fig. 1.2.4 shows an Atomic Force Microscope (AFM) image of $< 001 >$ $SrTiO_3$ after pulsed-laser-deposition growth of 11.3 layers of $SrTiO_3$ [44]. The Fourier transform of the AFM image, Fig. 1.2.4b, illustrates speckle in the diffuse 'Henzler rings' associated with the island structure. Using an incoherent beam with flux of 6×10^{13} photons/mm^2/s, the experimentally obtained diffuse scattering profile in Fig. 1.2.4c corresponds to the intensity in the white rectangle in Fig. 1.2.4b. The ERL will provide sufficient coherent flux to study dynamics based on the speckle seen in Fig. 1.2.4b.

Studies of ferromagnetic and ferroelectric domains and dynamics [45] will be greatly enhanced by the ERL's high-coherent flux and quasi-continuous time structure. Other real-time studies of interface-based processes can be imagined, such as grain-boundary evolution under load. It would be possible to study interfacial reactions under aggressive chemical conditions in reaction vessels, studies that are unfeasible by other methods. Interfacial structural analysis of small-grained materials, such as clays and zeolites, would provide insights into the mechanisms of geochemical reactions important for environmental science. The cumulative impact on surface science will be enormous.

1.2.7 Can we improve energy storage, photovoltaic, and photolytic materials?

Society is in an energy crisis driven by the need to limit carbon emissions while simultaneously meeting the energy demands of a growing population. Better electrical-energy storage is critically needed to match available wind and solar power to demand, and to make more efficient use of power distribution networks. Hybrid and all-electric vehicles are currently limited by the power and energy density of battery and super-capacitor technologies. Advances in anode, cathode and membrane materials will be required to make fuel cells viable for both mobile and stationary applications. Perhaps the greatest prize of all would be an efficient means of using sunlight to photolyze water into hydrogen and oxygen. Fuel cells, batteries, super-capacitors, and photolytic materials depend on complex chemical reactions that result in physical changes, often as a function of charge state. To understand such processes requires probes capable of *in-situ* analysis of electrodes and electrolytes. Frequently, the relevant reactions vary rapidly in time, occur at surfaces and interfaces that are structured at the nanometer level, and are buried deep in nested assemblies. More capable x-ray beams are recognized as necessary to improve and enable energy storage, photovoltaic, and fuel cell systems [46]. Improving photovoltaic and photochemical energy conversion systems will require the ability to probe nanometer structures and energy levels at surfaces. Observation of transient effects that occur on very rapid timescales will also be needed to understand dissipative processes and improve efficiency. Improvements in the efficiency of photovoltaic cells or the capacity of storage batteries and super-capacitors by even a small percentage would have enormous beneficial consequences for society.

Advantages of an ERL: A recent workshop on basic research for electrical-energy storage [46] made a strong case for submicron probes for *in-situ* analysis of catalytic and electrolyte materials in batteries, fuel cells, and photovoltaic cells (e.g., Grätzel cells[47, 48]). Understanding these complex materials will require the full arsenal of analytic tools, including advanced x-ray, neutron, and electron probes. But even this arsenal has limitations. Progress will require understanding structural changes and chemical reactions on sub-picosecond timescales in materials that are heterogeneous on submicron scales and buried deep inside active devices. The demands of *in-situ* measurement, often involving solvated environments and the need to track over time without destroying the nanostructure, precludes many electron microscope and XFEL methods. Work at an interface and/or at submicron size requires intense x-ray nanobeams that peer through solid layers and can be timed to a fraction of a picosecond, which limits the feasibility of storage-ring sources. In contrast, ERLs are better suited to this work and will be an enabling technology to study materials for energy storage and generation.

1.3 ERL Overview

In the next few sections, we give a brief introduction to ERL technology and to Cornell University's proposed ERL facility. The scientific facility described in this Project Definition Design Report (PDDR) will be a first-of-its-kind high-spectral-brightness, coherent source of hard x-rays. This source will enable a broad scientific program that goes well beyond what can be carried out with existing storage rings and is complementary to X-ray Free Electron Laser (XFEL) sources.

1.3.1 What is an ERL?

The fundamental difference between an ERL and a conventional storage-ring light source is that the electron bunch is used to make Synchrotron Radiation (SR) for a time much shorter than the characteristic damping time of the ring. Because of this, the phase-space of the particles, and the resulting SR light, are almost entirely shaped by the linear accelerator, and not by equilibrium storage-ring constraints. A photoinjector-Linac combination can flexibly produce extraordinarily high quality electron beams (e.g., bunches that are ultra-compact, ultra-low emittance, and with low energy spread), but these beams carry very high power: a 100 mA, 5 GeV beam has 0.5 GW of beam power. If this power had to be supplied continuously via wall-plug power, the machine would be impossibly expensive to operate. **The fundamental innovation of the ERL is that this beam power is recycled at near-perfect efficiency to accelerate new electron bunches.**

Figure 1.3.1 is a schematic of a 5 GeV ERL concept. An injector delivers very low emittance bunches of 15 MeV energy into the main superconducting Linac at a 1.3 GHz rate. The bunches are accelerated to 5 GeV in the main superconducting Linac and push past a weak dipole magnet into the return-transport loop. The transport loop hosts the undulators for SR production, as well as optional bunch compressors and decompressors for generation of very short ($\lesssim$ 100 fs) bunches along part of the loop. Bunches then return back into the Linac, but the loop-path length is adjusted so the bunches enter the Linac 180° out of accelerating phase. They decelerate through the Linac and emerge with the injector energy minus SR losses. These bunches have sufficiently low forward momentum that they are deflected by the weak dipole into a beam stop. The design allows for the filling of every 1.3 GHz RF period with both an accelerating bunch and a decelerating bunch, i.e., accelerating and decelerating bunches are interleaved in the Linac.

Superconducting radio-frequency (SRF) cavities are used to both accelerate and decelerate alternating bunches of particles, so the kinetic energy carried by the beam is recycled with near-perfect efficiency [49]. Because the spent beam's energy is recovered into the electromagnetic field of accelerating cavities, to be used for acceleration of a new beam, these cavities have to be filled with field continuously. A pulsed Linac as in the proposed European XFEL can therefore not be used. In order to have a reasonably short Linac, the accelerating field of the cavities must be rather high, and only SRF accelerators can simultaneously produce large

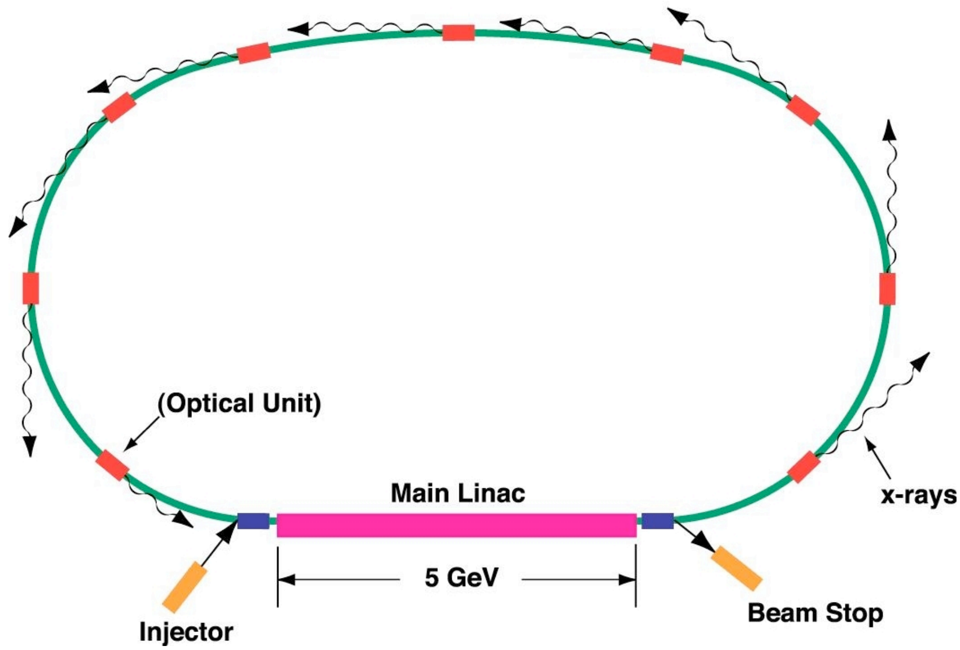

Figure 1.3.1: Schematic ERL facility consists (counterclockwise) of an electron injector, a superconducting Linac, beam stop, and transport-return loop-hosting undulators (red blocks) to generate beams of x-rays.

fields and continuous operation with the required negligible wall loss. The recent progress of high-field SRF cavities, therefore, makes this the opportune time to develop an x-ray ERL.

1.3.2 Overview of an ERL Upgrade to the Cornell Electron Storage Ring (CESR)

Several laboratories, most notably the Thomas Jefferson National Accelerator Facility (TJNAF), have demonstrated the feasibility of energy recovery for a low-energy particle beam [50, 51]. In 1999, Cornell scientists began exploring the possibility of building a high-energy, hard x-ray source using ERL technology, and by 2000 an international workshop at Cornell concluded that such a source would provide unique capabilities for x-ray-based science [52]. In 2001, a detailed Cornell/TJNAF study [53] began defining an ERL facility and pointed to the research and development needed to assess practical feasibility. NSF support for study of the underlying physics and technology began in February 2005. These studies apply to any ERL facility that may be built in the future. However, to work out the implications of a practical implementation of the ERL principle, an example is needed. The potential for applying the ERL idea to the existing CESR facility at Cornell provides the example used in [54, 55] and shown in Fig. 1.3.2. Study of any features of the design that are uniquely site specific, such as civil engineering, was supported by Cornell University and the State of New York. No NSF funds were used for this purpose. This accelerator concept has been presented at several international workshops, most notably at the Third International ERL Workshop held at Cornell in 2009 [56].

Referring to Fig. 1.3.2, a high-brightness injector system (0) delivers very low emittance

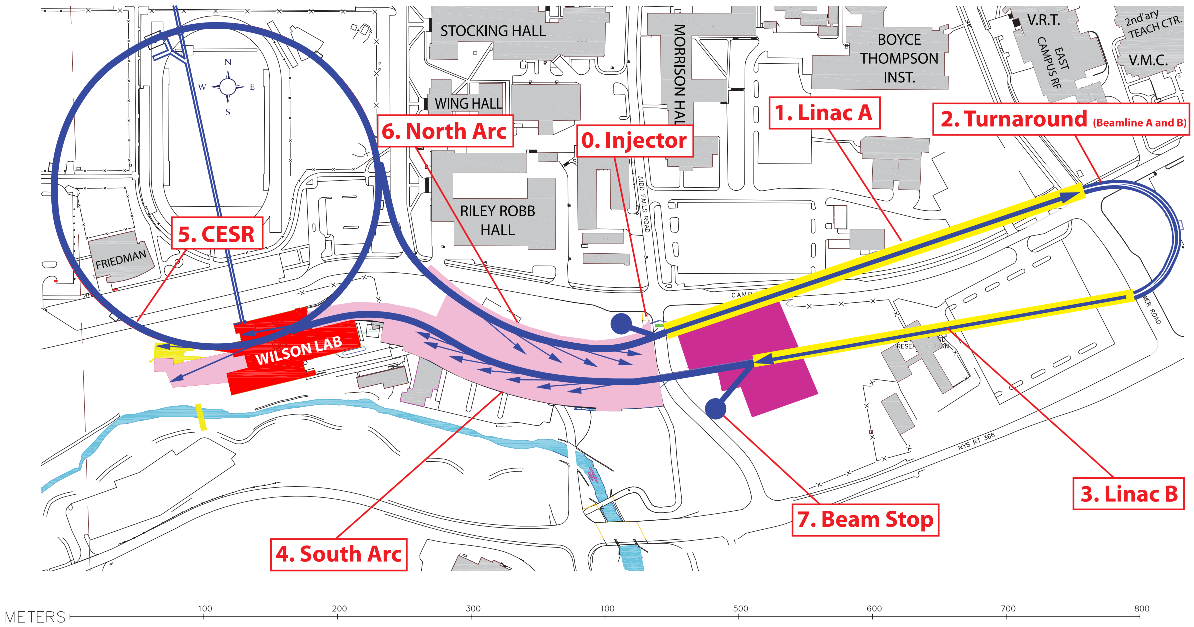

Figure 1.3.2: Schematic ERL layout incorporating the existing Cornell Electron Storage Ring (CESR). Electrons are injected (0) and accelerated to the right through a 2.7 GeV Linac (1), then looped through a turn-around arc (2), and accelerated to the left through an additional 2.3 GeV Linac (3) to 5 GeV. Beamlines are in the pink/red areas. Bunches then pass clock-wise around CESR (5). Bunches may be compressed to 100 fs (6) and feed more undulators before being uncompressed; their energy is recovered in second passes though Linacs (1) and (3). Finally they are stopped. Additionally a beam can be extracted after the second Linac (3) for bunch compression and novel radiation processes like the XFEL-O.

bunches of electrons into Linac A (1) at a 1.3 GHz rate. This rate is sufficiently high that even relatively low charge bunches (e.g., $\leq 77\,\mathrm{pC}$) provide a sufficiently high beam current (up to 100 mA) needed to generate a high average x-ray flux. The injector consists of a laser-driven photoemission gun coupled to a short superconducting Linac that accelerates the electrons to 15 MeV, at which point the electrons are sufficiently relativistic to largely prevent charge repulsion in the bunch from leading to emittance growth. Superconducting Linac A then accelerates bunches to 2.7 GeV, whereupon they enter a turn-around section (2), and then a superconducting Linac B (3). Linac B accelerates bunches to the 5 GeV operating energy of the machine. In this design, the Linacs and turn-around section are all housed in a deep underground tunnel that provides radiation protection and compatibility with the Cornell campus.

The south arc of the machine (4) conveys the electron beam though a series of undulators in a new x-ray experimental hall (shown in pink) that houses x-ray beamlines, schematically depicted as tangential arrows. The electrons then pass through more undulators in the existing Wilson Laboratory building (red) before being turned back around via the existing underground (5) CESR tunnel. The reuse of both the Wilson Lab and CESR further reduces costs.

The total cost of the here presented light source design has been studied in some detail, based on the studies provided as an online appendix. We do not yet present the cost study itself.

The electrons then enter the north arc (6) and the north side of the experimental hall, where there are more undulators and more beam lines. If desired, bunches may be compressed with chicanes to < 100 fs length for use in fast-pulse science in the north experimental beamlines. After exiting the beamline hall, the electron bunches decelerate first though (1) Linac A (1), pass through the turnaround loop (2) and further decelerate through Linac B (3). At this point, the bunch energy is that of the injector less synchrotron radiation losses of 2.5 MeV from dipole magnets and 2.5 MeV from undulator magnets, resulting in a final energy of ~ 10 MeV. These bunches are conveyed to the beam stop.

These numbers can be used to define ERL-power and ERL-current efficiencies. To control the cavity fields under realistic microphonic perturbations, 5 kW RF power will be installed for each cavity. The total RF power required to operate the ERL is approximately 3.4 MW (this is 1.5 MW for the injector and 384×5 kW for the Linacs). The EL produces a beam power of 500 MW and therefore has a power efficiency of about 146. Without energy recovery, the installed RF power per cavity would only allow the acceleration of a 0.38 mA beam, and therefore the current efficiency is about 260.

ERL designs are inherently flexible. For example, one can envision two injectors at (0) to provide flexibility and backup. In routine operation one of these devices may be used to produce large bunches (~ 1 nC) at low frequency (10 kHz) into the bunch stream from the other injector. These large bunches are accelerated via the Linacs and extracted from the south arc at the eastern end of the experimental hall (4) to a special 'extracted bunch' beam line (not shown) for accelerator physics experiments on XFELs, XFELOs or other short-pulse applications. Because these bunches arrive at low frequency, they have low average beam power and could be discarded after use without energy recovery. However, detailed considerations of multiple injectors and XFELOs are beyond the scope of this PDDR. They could be added at a later engineering design phase. Obviously, this is a future cost versus benefit decision that will depend on community interest and funding.

1.3.3 Outstanding features of the ERL design

Outstanding features of the ERL shown in Fig. 1.3.2 include near-full transverse coherence, small, round-source size, short native-pulse length, and high repetition rate as shown in Tab. 1.3.1 and Fig. 1.3.3. Additionally, the bunch structure can be tailored to specific x-ray experiments. Because an ERL has Linac-quality beams, the energy spread is very low and allows full utilization of a larger number of undulator poles than possible at a storage ring. Furthermore, an ERL does not require optimized electron optics for the large dynamic aperture needed for injection or for storage of beam for millions of turns. Consequently, the optics in ERL undulators is very flexible, and beam size and beam divergence can be fine tuned to experimental needs.

As shown in Tab. 1.3.1 the facility is very flexible and several dedicated running modes with specific bunch repetition rates and bunch charges could be provided. Here we specify the following three representative modes: (A) high-flux, (B) high-coherence, and (C) short-pulse, low-charge modes. Furthermore, using a fast kicker, the extracted bunch beam line (not shown in Tab. 1.3.1) mentioned above allows for simultaneous x-ray operation in any of the above

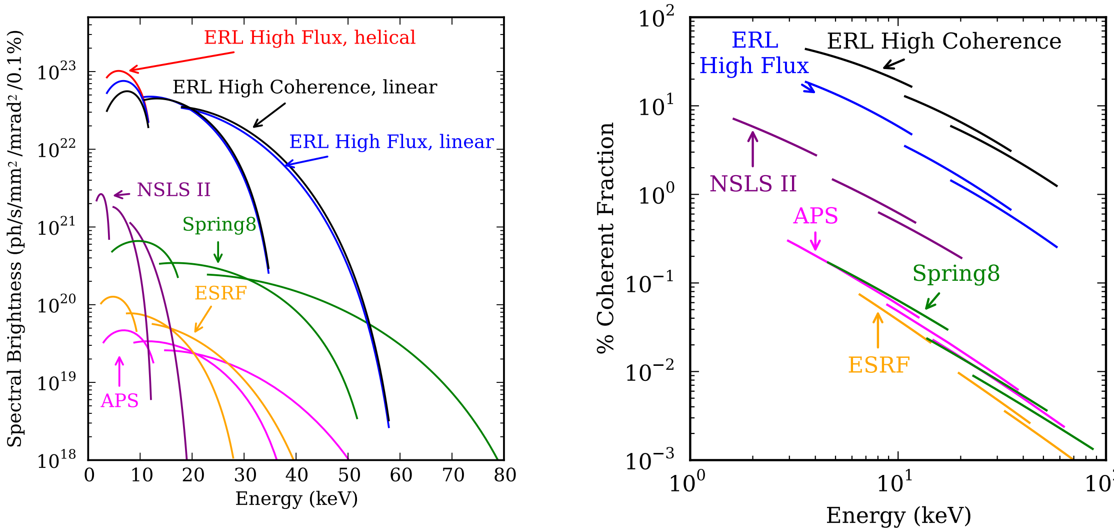

Figure 1.3.3: (Left) The average spectral brightness vs. energy for the 1) ERL in Hi-flux mode (5 GeV, 100 mA, 30 pm round beam, 22 mm period ID) and ERL in Hi-coherence mode (5 GeV, 25 mA, 8 pm round beam, 22 mm period ID). Even higher brightness may be feasible with advanced undulators or advanced beam collimation; 2) Spring8 (8 GeV,100 mA, 3.4 nm $\times$ 6.8 pm emittance, 3.2 cm period ID); 3) NSLS II (3 GeV, 500 mA, 0.55 nm $\times$ 8 pm, 14 mm period SC Undulator); APS (7 GeV, 100 mA, 2.5 nm $\times$ 20 pm, 3.3 cm ID). (Right) Coherent fractions for the various sources are indicated.

modes by plucking specific bunches out from the main stream at ≤ 10 kHz. The bunch charge can be up to 1 nC, in which case the geometric emittance (h/v) is simulated to be 2300/33 pm for an rms bunch duration of 100 fs and a relative energy spread of 2×10^{-3}.

Spectral brightness and transverse-coherent flux both scale inversely with the product of the transverse emittances, which is why the small emittances of the ERL are so significant. Small emittances also facilitate the production of intense nanobeams: Any electromagnetic radiation source is limited by the brightness theorem, which states that the beam area times the beam divergences (i.e., the brightness, for a given wavelength and number of photons in the beam) is at best, constant, no matter what passive, optical elements are inserted into the beam. Because of this constraint, microbeam optics invariably trade beam divergence for focal-spot size. The ERL has extraordinary brightness, allowing ultra-intense nanobeams.

Sub-micron x-ray beams have been a great success of third-generation SR sources [57–63]. However, storage rings are limited by beam emittances that are much larger horizontally than vertically, as shown in Tab. 1.3.2, thereby constraining the intensity to typically 10^{12} xrays/s/μm^2. The ERL has extraordinary brightness, allowing intense nanobeams. ERLs are nearly diffraction limited in both directions. With suitable x-ray optics, now under development at several labs, the potential exists for 1 nm hard x-ray beams with $\sim 10^{11}$ to 10^{12} xrays/s/nm^2 [64].

The one-pass nature of the electron trajectories in the ERL preserves the injector-beam

Table 1.3.1: ERL operating modes. Horizontal emittance ϵ_x, vertical emittance ϵ_x, bunch duration σ_z/c, and relative energy spread are results from start-to-end simulations in §2.1.15, incorporating space charge, incoherent and coherent synchrotron radiation, alignment and field errors, and orbit correction. SA and NA denote insertion devices the South Arc and North Arc. Note that for the 5 GeV beam, normalized emittances can be found my multiplying the geometric emittances below by about a factor of 10^4.

Operating Modes	A	B	C	Unit
	High Flux	*High Coherence*	*Short Bunch*	
Energy	5	5	5	GeV
Current	100	25	25	mA
Bunch Charge	77	19	19	pC
Repetition Rate	1.3	1.3	1.3	GHz
ϵ_x (SA/NA)	31/52	13/34	21/66	pm
ϵ_y (SA/NA)	25/26	10/10	14/14	pm
σ_z/c (SA/NA)	2.1/2.1	1.5/1.5	1.0/0.1	ps
σ_δ (SA/NA)	1.9/1.9	0.9/1.0	9.1/9.3	10^{-4}

Table 1.3.2: Comparative source sizes and divergences.

Machine	Note	Horiz. Size (μm)	Horiz. Div. (μrad)	Vert. Size (μm)	Vert. Div. (μrad)
ESRF	4 nm, 0.6 % coupling, ID13	59	90	8.3	3
APS	2.5 nm, 1 % coupling	275	11.3	8.8	2.9
NSLS II	0.5 nm, 2 % coupling	28	19	2.6	3.2
ERL	25 m und hi-flux, 30 pm	24.5	6.1	24.5	6.1
ERL	1 m und hi-coher, 8 pm	2	4	2	4

properties. The native-bunch duration from the electron photoinjector of approximately 2 picoseconds is already much shorter than existing storage ring sources and will be available simultaneously to all x-ray beamlines at an ERL. In addition, magnetic bunch compressors could be used to provide much shorter pulses at selected stations as noted in §2.1.10.

ERL technology is young. The parameters presented in Tab. 1.3.1 may be expected to improve as the technology develops. The proposed ERL at Cornell is, thus, an accelerator with a potential for further improvement, especially in the injector area where an improvement in the injector brightness will directly translate in an improvement in x-ray beam brightness. It is envisioned both as a user facility and a test bed for ERL light source technology. The development of ERL technology is also timely. Synchrotron radiation is a hotly competitive field internationally, and many believe that the U.S. lead in SR research is eroding. U.S. leadership in ERL technology will very much depend on whether or not a decision is made to build a facility such as the one described in this PDDR.

1.3.4 Cornell's location for an x-ray ERL

This PDDR is a technical analysis of a full-scale hard x-ray ERL facility. An in-depth analysis requires details about a site, since the site determines many aspects of the machine and facility construction. This PDDR assumes a site with which we have the most familiarity, namely, the site of the current x-ray synchrotron source at Cornell University. There are many advantages to choosing the Cornell site for a detailed study. For example, we have enough geotechnical information about our site to work though complex considerations of tunneling procedures, ground vibrations, and constraints of civil construction. Although it is hoped that such a facility would be built at Cornell, the PDDR is a valuable contribution even if some other site is chosen, for two reasons: First, much of the PDDR is not site specific. Second, in cases where site-specific information was required, the selection of a site brought quantitative, real world considerations into focus. Thus, the PDDR sets a benchmark for depth of analysis that must be considered for an ERL project to be successful. This having been said, it will be obvious that one could not resist the temptation to explain, along the way, why Cornell University is a uniquely excellent site for an ERL facility.

The x-ray ERL described herein is designed to make optimal use of existing facilities at Cornell's Wilson Laboratory. This has numerous advantages: Reusing almost a kilometer of tunnel, magnets, and much of the infrastructure of Wilson Laboratory has considerable cost savings. The central campus location provides low-barrier access to the staff and students who are training in x-ray and accelerator science and technology, a feature that has been key to the success of the Cornell Laboratory for Accelerator-based ScienceS and Education (CLASSE). The G-line facility at the Cornell High Energy Synchrotron Source (CHESS) National Facility, the majority of the CESR storage ring, and the entirety of the Wilson Laboratory and infrastructure are incorporated into the plan. Making use of the existing infrastructure is worth several hundred million dollars. Referring to Fig. 1.3.2, Wilson Laboratory is imbedded into a hillside between the Cornell campus to the north and Cascadilla creek to the south. The CESR tunnel is approximately 15 meters below the soccer field to the north of Wilson Laboratory. With a creek to the south and buildings to the west and the north, the ERL's Linacs extend to the east and connect to CESR as shown in the figure. An extension in this direction is particularly suitable because it leads the Linac along a section of a hillside out of which x-ray beamlines can be directed to an experimental hall.

The existing infrastructure of Cornell's accelerator laboratory is reused to a large extent. CESR has been designed for 8 GeV electron and positron beams. The magnets are therefore strong enough for the 5 GeV ERL beam, even though this beam requires relatively stronger magnets to control its parameters tightly. The magnets of 75% of this accelerator, their vacuum chambers, and their magnet stands would be reused for the ERL. The G-line building is the latest extension to the CHESS experimental area and the ERL design expands utilization of this area through construction of a new G-line Annex. Furthermore, the ERL would continue to use the full Wilson building for accelerator and x-ray scientists, outside x-ray users, machine shops, a vacuum laboratory, magnet metrology, and similar support facilities like cooling towers and megawatt transformer pads.

The proposed new beamline hall to the east of Wilson laboratory, together with the Linac tunnel, has been designed by the international engineering firm, ARUP. Its initial design has been subjected to value engineering, resulting in a refined Project Definition Design [65, 66].

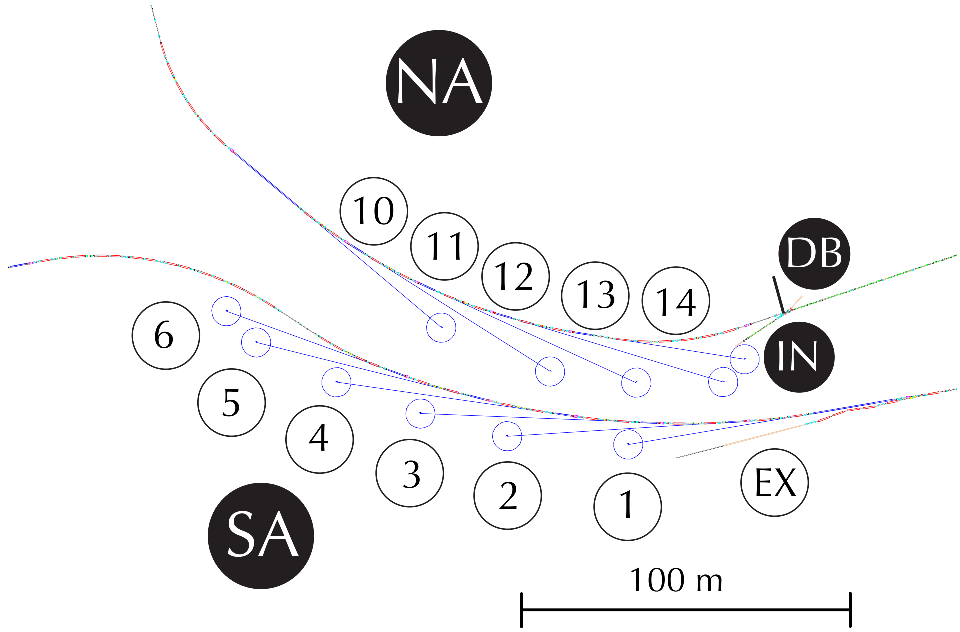

Figure 1.3.4: Layout for x-ray beamlines in the new user hall east of Wilson laboratory. Here IN is the injector, DB is the diagnostic beamline, NA is the north arc, and SA is the south arc. Numbers indicate x-ray beamlines. Beamlines 7–9 are in Wilson laboratory, G-line Annex, and G-line respectively. EX is the extracted beamline.

A high-level summary is presented in Chapter 4. The accelerator tunnel has also received attention from an Underground Tunnel-engineering Advisory Panel (UTAP) of world-renowned tunnel experts [67], whose recommendations have led to cost-effective parameters for the tunnel diameter, the layout curvature and the housing of each of the two main Linacs in separate tunnels. The suitability of the tunnel location has been verified by a series of test borings all along the tunnel path [67].

Another infrastructure component required by the ERL is a large cryogenic installation for liquid helium. The energy recovery principle of using the spent beam's energy for accelerating new particles allows much larger beam current than available in conventional linear accelerators. However, this involves cooling superconducting Linacs to liquid helium temperatures and requires a large cryogenic facility. A suitable location for this has been determined and a building has been designed. The two major international cryogenics companies have delivered layouts and cost estimates for the full cryoplant system.

Superconducting accelerators and beamlines are very sensitive to vibrations. Ground vibrations at the ERL location have therefore been studied by an engineering firm and by Cornell scientists [68, 69]. These studies confirm that the proposed location is suitable for the proposed ERL facility.

1.3.5 ERL design and layout

The accelerator's layout is determined not only by architectural and tunnel-engineering considerations but to a larger extent by accelerator technology, beam physics, and x-ray needs. Limits on available magnet strengths, permissible heat loads on chamber walls that are exposed to synchrotron radiation, the power density of this radiation, the emittance and energy-spread increase in tight or too long bends, and similar technical considerations have influenced the design of the layout. Chapter 2 of this PDDR describes design choices that make cost-effective use of this suitable location for an ERL by:

- Utilizing most of Wilson Laboratory's accelerator and x-ray infrastructure
- Providing 14 x-ray beamlines with easy access as shown in Fig. 1.3.4
- Having two buildings (east and west additions) to house all x-ray beamlines outside of Wilson Laboratory as well as the ERL injector
- Accommodating three 25 m long undulators

The choice of 14 beamlines, each of which can host a number of stations, is a cost consideration. More beamlines are feasible if the main beamline hall is extended to the east, but our present thinking is that the cost of doing so does not justify the expenditure. This is one of many issues that can be re-addressed during the Engineering Design Phase.

The international accelerator technology company, Research Instruments GmbH, (formerly ACCEL) has provided a cost estimate for the construction and installation of the warm accelerator components [70]. The companies Air Liquide and Linde have analyzed the cost of the cryogenic Linac and the cryogenic infrastructure [71, 72]. For both, a detailed design for the accelerator has been required to make sure no relevant aspect of charged-particle optics and beam dynamics has been overlooked. The design therefore contains considerable detail in determining the lengths of all magnets; providing space for all beam instrumentation, beam-orbit correctors, vacuum flanges and gate valves; determining power supply strengths and stability; limiting magnetic field errors and limiting placement errors. All these details have small but significant consequences in the cost and for the layout. This PDDR describes beam-dynamics effects considered in the design, and demonstrates the choices made to reach desirable accelerator performance. Examples of such choices are the following:

- Providing sufficient space in the user hall for the injector, a diagnostics line to optimize its performance, and a second injector for upgraded operation, if desired.
- Having two turn-around loops in the east can provide different energy-dependent time-of-flight for the accelerating and decelerating beams, reduce the beam energy spread, and require a sufficiently large-tunnel cross section.
- Locating a beam stop directly after the south Linac in a radiation-shielded spur off the main tunnel provides a beam-stop that can accept a beam with unusually large energy spread.

- Collimators to control beam halo, to act as undulator protectors and soft bends for controlling bremsstrahlung background all require sufficient space, restrict the places for sensitive electronics, and determine space needs around undulators.
- Preferences of x-ray users for the lengths of x-ray beamlines, for hutch space, and the need to have x-ray optics outside a shielding wall no more than 30 m after the undulator determines the width of the user hall, the curvature of its walls, and the number of undulator beamlines.
- Requirements for technical components, e.g. power distribution, water-cooling, cryogenic distribution, and air-conditioning also influenced layout and construction choices.

Section 2.1 describes the physics and cost considerations that have lead to these and other design choices.

The ERL described in this PDDR is located within a vibrant scientific community at Cornell. It is close to faculty and students who use it and close to collaborating scientific facilities, such as Cornell's nano-fabrication center. It extends an existing accelerator installation, reusing its infrastructure, and it upgrades the CHESS x-ray laboratory. Its location is suitable with respect to ground vibrations, sufficient space for an experimental-user hall, a large cryogenic infrastructure, and an accelerator tunnel. The layout is compatible with accelerator-technological and beam-dynamical restriction, and it takes into account considerable details of an accelerator design that can provide the short x-ray pulses of high spectral-brightness that distinguish an ERL x-ray source.

Cornell has decades of experience with Wilson Laboratory as the site of an international-user facility and locus for national collaboration. Cornell has advantages of being both remote and connected at the same time. It is sufficiently remote that residents, users, and visitors can focus on research with few distractions. At the same time it is within ten minutes from a regional airport connecting to New York City, Philadelphia, and Detroit, and just over an hour by car from the Syracuse airport. Cornell is within a working day automobile range from most of the northeastern United States and the major Canadian cities of Toronto, Ontario and Quebec. The experiences of the Elementary Particle Physics (EPP) CLEO collaboration of 22 universities, which was a major activity at Wilson Laboratory for 30 years, and of CHESS as one of the five National hard x-ray use synchrotron facilities has proven that Cornell is a suitable location.

In short, not only is Cornell ideally situated for the proposed ERL, but it has a well-developed and cost efficient design adapted to its environment, and has pursued cutting-edge x-ray and electron beam research.

1.4 Timeline

1.4.1 ERL developments

Many technologies had to be examined and developed prior to a detailed engineering design of an ERL facility. Superconducting RF-cavity technology and ultra-low emittance sources lead this list, closely followed by emittance-preserving transport, highly stable RF-control systems, extremely smooth-surfaced vacuum systems to minimize growth in energy spread, new concepts for insertion devices, x-ray optics, and control of radiological effects to name a few.

Cornell has been a leader in superconducting RF technology for many decades, and maintains an active development and engineering effort in this area. While the greater part of the work to build an effective RF accelerating cavity has been done during recent years, configuring the cavities to serve efficiently in an ERL and providing a suitable cryostat.

The original ERL emittance target of the Phase 1a program was only $2\,\mu$m for 77 pC per bunch, and this goal was achieved a few years ago. The subsequent Phase 1b program has pushed the envelope down to a goal of $0.3\,\mu$m. At the time of this document, there ERL team has achieved $0.3\,\mu$m core emittance, while 100% of the beam is within a $0.8\,\mu$m emittance. This is already better than the horizontal emittance of all existing storage-ring facilities. Accelerating a beam with these emittances would already produce an x-ray beam brighter than any existing storage-ring source. This brightness would require horizontal and vertical emittances of about $0.6\,\text{mm} \times 0.6\,\text{pm}$ or about $50\,\text{pm} \times 50\,\text{pm}$ in an ultimate storage ring with a 100 mA beam.

Emittances are expected to further improve during the remaining Phase 1b research and development. Components that have contributed to this success include suitable photocathodes and laser systems, a high-voltage, low-emittance gun with appropriately controlled bunch-dynamics, RF source with precision phase and amplitude control, RF cavities and supporting cryomodule, and diagnostics to evaluate and control the beam transport. Every component of this system has been carefully designed for emittance preservation and stability.

In 2001, Cornell organized the first x-ray and accelerator sciences workshop for an ERL. At that time the most pressing questions that remained about x-ray ERL technology were identified and a prototyping facility was proposed at Cornell to address these issues. Some of the questions were addressed in collaboration with the Thomas Jefferson National Accelerator Facility, and others have been investigated at Cornell's ERL completed Phase 1a prototyping facility.

The second stage of research and development (Phase 1b) is now underway, with 1.5 years remaining at the time of this document. It has used the hardware of Phase 1a to achieve the following:

- To verify that photocathodes have sufficient lifetime to provide a 100 mA electron current for prolonged periods of time, the Cornell photoinjector prototype has demonstrated record lifetimes from K_2CsSb photocathodes having operated 20 mA for 8 hours without any noticeable degradation of the photocathode's quantum efficiency.
- A record high average current of 52 mA has been achieved from a GaAs photocathode, including a clear path towards realization of stable many-hour operation at these current levels.
- A high-power fiber laser operating at 1.3 GHz was built and has operated as high as 60 W average power at 520 nm. A 1% quantum efficiency cathode requires 20 W of light to generate 100 mA, and 2 W for a 10% QE cathode, so we have successfully demonstrated a laser system with sufficient power and stability for our ERL design.
- To verify that the beam dynamics can be controlled well enough to produce emittances that realize an ERL's potential, the Cornell photoinjector team has experimentally

demonstrated a record beam brightness from the electron source with the final beam emittance largely dominated by the thermal emittance of the photocathode and, therefore, conducive to further improvements as better photocathode materials become available. A 90% rms normalized beam emittance of $0.5\,\mathrm{mm}\cdot\mathrm{mrad}$ has been achieved for the goal specification of 80 pC/bunch and $0.2\,\mathrm{mm}\cdot\mathrm{mrad}$, 90% rms normalized beam emittance for 20 pC/bunch.

- Cornell is in the process of building a prototype ERL cryomodule to determine a realistic construction cost for this major accelerator component, to determine microphonic noise that strongly influences the RF power requirement of the ERL, and to determine dark current and x-ray background that influences costly shielding of RF equipment in the ERL tunnel. As of Fall 2012, the design of the cryomodule is completed and its six cavities are being constructed.
- The construction of these six cavities will verify that cavities with a quality factor Q_0 of 2×10^{10} at accelerating voltages of 16 MV/m and temperatures of 1.8 K can be produced with a high success rate. As of fall 2012 only one ERL cavity has been completed, and it tested successfully, fulfilling all its requirements.
- Microphonics levels in a one-cavity test cryostat lead to a loaded Q_L of 6×10^7 and 5 kW power per cavity. If microphonic cavity detuning is smaller in the ERL cryomodule, then Q_L could be made larger and the power sources and couplers could be reduced in size and cost.
- A one-cavity test cryostat has been equipped with a 7-cell ERL cavity and will be placed after the prototype ERL injector. This will show whether the HOMs that the 100 mA beam excites are sufficiently damped to avoid the beam-breakup (BBU) instability.
- A 20 cm prototype ERL undulator has been built and tested successfully with electron beam. The LCLS has adopted the delta type of the ERL undulator as end stage of its beamline to produce intense circularly polarized beams. This construction provides a realistic costing and verifies the tolerances that can be maintained.

1.4.2 Engineering design and timeline

The Phase 1b research and development is expected to run though March 2014, but many questions will be answered much earlier. Photocathodes, electron gun, and SRF injector Linac studies are already under way. The full construction cost of an ERL cryomodule/cavity assembly will be determined well before testing is complete, and several cavity properties (e.g. Q_0) will have been determined on a horizontal test stand.

Given funding, engineering design for the Cornell ERL can commence now, and Phase 1b studies can be completed subsequently. Indeed, as for any large facility, the engineering and design for the Cornell ERL must begin well before construction. Final architectural designs, component designs, industrialization of the Linac and other large components, and requests for proposals for major systems should be completed by the start of construction. Smaller components (e.g., magnet power supplies and computer systems) may be completed during the first couple of years of construction.

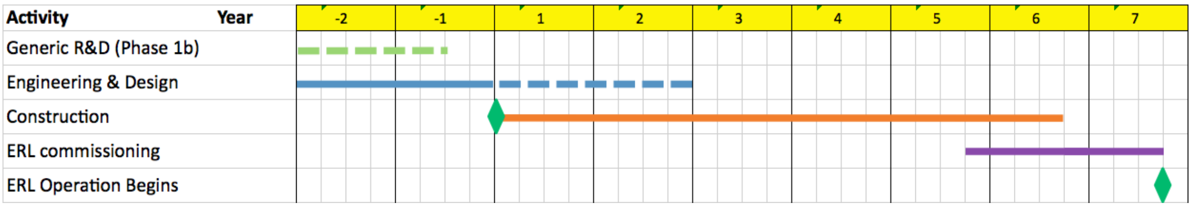

Figure 1.4.1: Timeline for ERL Phase 1b research and development, engineering design, and construction in calendar years. We believe that construction could be started as early as January 2014.

The successful development, construction and commissioning of a large facility, like an ERL, requires both a complex infrastructure and a collection of people with skills that takes many years to assemble. Continuity is essential. Once suitable personnel are assembled, they cannot simply be put into hibernation for a few years and then resurrected. Cornell has assembled such individuals over the past several decades and who are now simultaneously engaged in ERL research and development, operation of the CHESS facility, and maintenance of the CESR accelerator complex. Obviously, decisions about final construction are contingent upon continued successful progress of the research. However, realities of the calendar dictate that this cannot simply wait until the research is completed. For this reason, every major new type of synchrotron machine that has ever been built advanced simultaneously with requisite research and development. What is reasonably required well in advance is confidence that technical issues can be addressed within well-defined costs and time frames, a case that is made in this PDDR.

As described in Chapter 4, ARUP, the international engineering firm, has produced three volumes of an extensive report about civil construction and infrastructure [65, 66, 73]. The third volume takes into account a detailed analysis of the tunneling and other earthworks, as well as the time it would take to construct a low-vibration user area.

A reasonable transition from Phase 1b research and development over engineering design to ERL construction with appropriate overlap periods is shown in Fig. 1.4.1.

1.5 Historical NSF, New York State, and Cornell Context

1.5.1 NSF Light Source Panel Report

In 2007, the NSF Mathematics and Physics Sciences Directorate (MPS) assembled a panel of experts chaired by Venkatesh Narayanamurti, then Dean of Harvard's School of Engineering and Applied Sciences, and Cherry Murray, then of Lawrence Livermore National Laboratory and incoming president of the American Physical Society to examine the case for an NSF-stewarded fourth-generation synchrotron light source [74]. The charge to the panel was three-fold:

- What is the current view of opportunities for future research using major advanced light source facilities, and what facilities are envisioned to carry out such research in the U.S.?
- What does the Panel see as the most effective role for the NSF in helping to develop,

construct, instrument and operate such facilities?

- Do university-based light sources now under discussion in the community (for example, a soft x-ray Free Electron Laser and/or an Energy Recovery Linac) have a critical role to play in realizing the opportunities?

The panel spent the next year conducting an extensive examination of background materials, interviewing the community, holding workshops and visiting Department of Energy (DoE) and university-based light sources. The panel findings [74], delivered to the NSF MPS Advisory Committee (MPSAC) in the fall of 2008, opened with the following Executive Summary:

> Coherent, ultra-short pulse, exceptionally high brightness x-ray sources (so called 4th generation sources) have properties that far surpass those of current x-ray sources. The laser-like properties of these new sources promise to open up new scientific frontiers such as lens-less imaging and ultrafast dynamics and spectroscopy. Applications span an exceptionally broad array of scientific and engineering disciplines. There is strong, world-wide interest in the development of these sources especially in Europe and Japan, and the United States needs to move more aggressively in this new era. NSF-supported, university-based light source facilities have historically played, and are now playing, a vital role in advancing the state of the art and in education and training of the next generation of scientists and engineers. University-based light source developments currently under discussion such as the Energy Recovery Linac (ERL) and the soft X-ray Free Electron Laser (XFEL) have a critical role to play in realizing the opportunities afforded by 4th generation sources. The Panel recommends that NSF play a stewardship role in the design, construction and operation of university-based 4th generation light sources.

The Panel examined the science case for these machines and found it to be compelling (emphasis is from the Panel report):

> A new era of light source development is underway that will lead to significant improvements in the coherence properties of photons on a sample. These improvements will make practical novel methods for imaging and for probing of sample dynamics... **Exciting new scientific frontiers in areas such as lensless imaging, and ultrafast dynamics and spectroscopy are enabled by these properties. Exploiting this scientific frontier in the US is essential for our competitiveness in strategic areas of science, engineering, workforce development and could have significant commercial impact.**

In this regard, the Panel was aided by a science case that had been detailed many times in justifications for facilities such as PETRA-III, NSLS-II and MAX-IV [73-75]. The Panel then examined and listed the many accelerator and beamline physics research and development challenges towards developing a coherent light source. While noting the risks involved, it stated that training the requisite human capital to develop, build and utilize a coherent-synchrotron light source is a necessary part of the overall development (emphasis from the Panel report):

> **The NSF has a culture that particularly values high risk, innovative, leading edge research. Historically, university research has been a major source of new designs for light sources and associated experimental**

> **techniques. Accordingly, the panel suggests the challenges listed above are well suited to the NSF university facility environment, which offers students and post-graduate researchers significant opportunities in advancing accelerator physics and photon science.**

The report concluded with several findings:

> **Coherent, ultra-short pulse, exceptionally high brightness x-ray sources have properties that far surpass those of the current generation of x-ray sources.**
>
> **The scientific areas impacted are increasingly multidisciplinary and include biology, chemistry, physics, medicine, earth and environmental sciences, archeology, materials, physics and engineering. Interdisciplinary interactions will be greatly enhanced.**
>
> **Exploiting this scientific frontier in the U.S. is essential for our competitiveness in strategic areas of science, engineering, workforce development and could have significant commercial impact.**
>
> **There is a strong science case for 4^{th} generation light sources to be built in the U.S. in the next 10 years.**
>
> **NSF has the capability to design, construct and operate a 4^{th} generation light source as its steward and it is appropriate for NSF to do so.**

The panel specifically examined two next-generation light-source technologies, a hard x-ray ERL and a soft x-ray seeded XFEL. It noted: "However, ERLs and FELs have rather different source characteristics and as presently conceived, offer somewhat different x-ray properties in such areas as overall pulse structure and generation of VUV/soft or hard x-ray" and that pursuit of the science uniquely served by each "…may require two separately optimized 4^{th} generation sources."

Since the release of the Light Source Panel Report, the DoE has made substantial progress towards the design of a soft x-ray-seeded XFEL, with a detailed conceptual design emerging from the Lawrence Berkeley National Laboratory (LBNL). A recent comparison of the relative merits of ERLs and XFELs for coherence applications is presented in [8]. While no funding decision has been made, LBNL is clearly the front runner in the U.S. for a soft x-ray seeded XFEL. In the meantime, Cornell has made excellent progress on the ERL, as summarized in this report. The NSF has yet to decide if it will open a competition suitable for an ERL facility.

1.5.2 Cornell Phase 1 ERL research and development

Cornell University proposed a research and development plan towards a hard x-ray ERL to the NSF in 2001, which was favorably reviewed in 2002 by a joint Division of Materials Research (DMR) and Physics Division (PHY) review committee. The funding climate at the time was difficult, which introduced delay and necessitated breaking the project into two smaller, sequential pieces. The first, dubbed ERL Phase 1a research and development, was funded in 2005 as an NSF multi-divisional project [75]. The research and development encompassed many studies necessary for an ERL, especially the successful fabrication of the ERL electron injector. The injector is the most critical component, as it has to produce electron bunches of emittance sufficiently low to allow nearly full transverse coherence of the photon beam.

Full-scale optimization of the injector, as well as main Linac design, and other requisite developments, dubbed ERL Phase 1b research and development, were proposed to the NSF in the fall of 2007. It was reviewed both by mail and by a large panel of experts in the fall of 2008. The review examined both the science and technical cases for a hard x-ray ERL, as well as the progress of the Phase 1a research and development. The review was very favorable and full funding was recommended. Excerpts from the review summary follow:

> This proposal to carry out research and development in support of the ultimate construction and operation of an energy recovery Linac (ERL) at Cornell strives to create an x-ray light source with brightness and coherence properties superior to any existing storage ring light source. The team, largely composed of current CHESS staff but including additional Cornell faculty and partners worldwide, represents a very strong contingent of scientists and engineers with the insight, talent, and energy to carry out the work. Buoyed by strong support from NSF, Cornell, and New York State, this team is in an excellent position to carry out the proposed research as well as act as the intellectual driving force behind the ultimate construction of an ERL. To the best of our knowledge, all of the proposed studies are on the critical path to the eventual fielding of an operational ERL.
>
> The proposed ERL, when operational, would enable a very broad range of science, a good deal of which will be transformational. In opening up a new window for the study of materials, the ERL will make possible the discovery of new phenomena that will, at least in some cases, lead to paradigm shifts, resolve long standing questions, and initiate whole new fields of investigation. The ERL technology has obvious immediate advantages for hard x-rays and has enormous benefits to accelerator science generally.
>
> The proposal is well-considered, is supported by a dynamic young staff and demonstrates tremendous buy-in from the community. This proposal should be a top priority for funding, regardless of whether the ERL project is ultimately built at Cornell. It is a technology that is critical to develop, the CHESS group is ahead of everyone else in the world, and it is an area that can put the U.S. back in a leadership position.

The Phase 1b research and development has been funded through early 2014 [76, 77].

1.5.3 New York State and Cornell support

In 2006, the State of New York awarded Cornell four years of support totaling $12 million, augmenting several million dollars from Cornell, to develop a full-scale ERL facility design as an upgrade to the existing Cornell High Energy Synchrotron Source (CHESS) National Facility. This enabled development of the present PDDR by giving support for studies that fell outside the scope of the NSF ERL research and development awards, e.g., civil construction studies, tunnel studies, cryoplant studies, environmental studies. Ultimately, it is hoped that New York State will be a partner in a full-scale ERL facility at Cornell.

1.5.4 Historical Cornell context of CLASSE

Cornell has had an enormous impact on the accelerator-based sciences, arguably as significant as any other leading laboratory in the world. Accelerator-based research at Cornell is the result of a very productive collaboration that has been going on for the better part of a century between accelerator physicists, elementary particle physicists, and x-ray scientists. The practical beginning of synchrotron radiation science may be dated back to 1952 when Cornell physicists, who were building an electron synchrotron for elementary particle physics (EPP) purposes, collaborated with condensed matter physicists to build the world's first synchrotron radiation beamline to characterize and apply the radiation to the study of matter [78–81]. Over the next three decades, a succession of larger and more capable accelerators were built, each in turn contributing to both EPP and synchrotron studies. In the mid-1960s, the present Wilson Laboratory site was constructed to house a 12 GeV synchrotron and the associated experimental facilities. In the mid-1970s, the NSF Physics division (PHY) funded the addition of the Cornell Electron Storage Ring (CESR) for EPP, and the NSF Division of Materials Research (DMR) funded a national synchrotron radiation facility (CHESS) using the radiation produced by CESR [82]. CHESS and CESR commenced facility operations in 1979 and, with numerous upgrades, are still operating today. The complex has made many world-class contributions to EPP, accelerator, and synchrotron x-ray sciences.

The present synchrotron complex is managed by the Cornell Laboratory for Accelerator-based ScienceS and Education (CLASSE), which is a collection of faculty from several Cornell departments. Accelerator physics and x-ray science at CLASSE are intimately connected. The mission of CLASSE is to conduct research and apply accelerators and related technologies for synchrotron x-ray science and elementary-particle physics applications, and to educate the researchers involved. CLASSE operates the largest university-based accelerator complex in the U.S., a facility comparable in scope, size, and complexity to the largest x-ray synchrotron laboratories operated by the Department of Energy. The facilities in Ithaca include: (1) the Cornell Electron Storage Ring (CESR), a 768 m circumference, 8 GeV storage ring, typically operated at 5 GeV with up to 400 mA per beam; (2) a similar circumference synchrotron that serves as a full-energy injector into CESR (3) the CHESS x-ray facility; (4) the ERL Phase 1 injector facility, and (5) a superconducting accelerator test and fabrication facility.

Accelerators are large and complex machines, and require a substantial infrastructure of necessary technical skills (accelerator physics, vacuum, electronics, computer, safety, mechanical etc.), as well as an administrative organization capable of dealing with large-scale, nationally used facilities. This infrastructure, which has been working effectively at Wilson Laboratory for many decades, was reorganized and renamed CLASSE in 2006. CLASSE consists of an overall infrastructure led by a directorate, with directorate members leading subgroups devoted to various essential aspects of elementary particle physics, accelerator physics, and x-ray science. The directorate is informed by external advisory committees appointed by Cornell that report to the university administration and the funding agencies. CLASSE includes a full complement of dedicated shops and facilities that are required for a major accelerator laboratory.

The CLASSE organization allows the participants to engage in large, long-term projects that require the broad infrastructure of a complete laboratory. The Cornell High Energy Synchrotron Source (CHESS) and the now decommissioning CLEO EPP collaboration are examples of highly successful projects that have existed for decades. The ERL project is relatively young by this measure, having commenced at Cornell in 2000.

Given its broad scope, it is instructive to compare CLASSE to laboratories run by the Department of Energy (DOE). How CLASSE differs from a DOE laboratory is very relevant to understanding this document.

First and foremost, CLASSE is a university laboratory staffed by about 200 employees, and has a very flat, faculty-driven administrative structure that is not appointed by a funding agency. This small size and flat structure gives CLASSE great independence and flexibility to pursue research opportunities. Second, education and research are both equally important missions. Students are far more heavily involved in long term projects by virtue of the fact that CLASSE is an integral part of the Cornell campus. For example, graduate students in CLASSE routinely build and maintain accelerator and upstream portions of x-ray beamlines inside the primary shielding walls, in ways not allowed at DOE accelerator facilities. In this way CLASSE creates an important synergy with the national laboratories by training a disproportionately high fraction of the accelerator physicists and x-ray beamline scientists who later go on to build and run other national facilities.

A full-scale x-ray ERL would upgrade the CHESS facility by incorporating the storage ring and existing facility infrastructure into the ERL facility. The ERL facility is described in this PDDR as follows: Chapter 1: Introduction and Overview; Chapter 2; The Accelerator; Chapter 3: X-ray Beamlines; and Chapter 4: Civil construction and conventional facility aspects.

1.6 Scope of this Project Design Definition Report (PDDR)

Several questions naturally arise when considering a scientific facility: What is the scientific justification for the facility? What is scope and technical feasibility of building the facility? What specific experimental beamlines should be built? The approval and budget processes are slow and would take years. This is sufficiently far in the future that considerable community evolution is to be expected. Hence, this PDDR should give great attention to questions that can be reasonably answered now and less attention to aspects that are likely to evolve over the next few years.

Chapter 1 has presented the historical background and motivation for an ERL x-ray facility.

Chapter 2, which covers the accelerator system, comprises the bulk of this PDDR. There is confidence in the community that, if the (already funded – see §1.4.1) ERL Phase 1b injector successfully produces the predicted beams, then a coherent hard x-ray ERL facility is possible. However, there are still many issues of practical implementation, feasibility, and cost to be resolved. What are the requirements for stability of the accelerator and the building, and how may these be met? What are the requirements of the accelerator RF system and how may these be met? What are the requirements on the cryogenic system and how may these be met? Similar questions apply to the tunnel, the magnets, the electrical system, etc. In these cases, reasonable projections may be made **now** that would determine the facility scope and cost. Chapter 2 systematically addresses these areas.

Chapter 3 is concerned with the x-ray beamlines, which requires a different approach. Many of the questions that arise about beamlines are already being intensively worked on by the community for projects that will proceed rapidly over the next few years, e.g., PETRA-III, NSLS-II, and the APS and ESRF upgrades. For the sake of argument, assume that construction of the ERL will start in 2014 and take 5.5 years. Completion of civil construction to the point of initiation of installation of beamlines would not start until 2017 or 2018, by which time one expects huge advances to have occurred in x-ray optics and detectors. These advances would impact the specific beamlines that would be built. Importantly, experience gained at PETRA-III, NSLS-II and with the ESRF and APS upgrades will materially impact the specific practical implementation of the beamlines. Hence, it is wise at this point in time to refrain from being too prescriptive about the specific beamlines. On the other hand, a generic model is useful for costing purposes. Consequently, the goal of Chapter 3 is to present a 'strawman' model of specific ERL-type beamlines, and a list of beamlines that would be built if construction were to commence tomorrow.

A second reason to defer detailed specification of the beamlines is that beamline definition is a community activity. Beamline definition will involve coalescence of teams of scientists from many institutions around specific science areas, typically via focused workshops. Cornell engaged in precisely this type of activity with the 2006 ERL summer workshops [83]. This process needs to be repeated every few years because synchrotron radiation is a very rapidly progressing field. Accordingly, Cornell, along with partners at KEK (Japan), SSRL, DESY (Germany), and others will hold a new set of workshops in June, 2011 [84]. The outcome of these workshops will be the next stage in the process of both defining the most attractive science areas and in defining the best beamline configurations to perform the science. Indeed, the NSF Light Source Panel report [74] recognized that the ERL beamlines must evolve with the user community:

> Since the ultimate goal of the next-generation light sources is to address transformational science, the user research communities must be involved from the beginning in developing the facility specifications and design. To help communication, it is advantageous to continue active user research programs where next-generation light source research and development work is being pursued.

Chapter 4 is concerned with civil construction and conventional facility aspects. Cornell partnered with the State of NY to fund detailed architectural and engineering studies performed by ARUP, an internationally known engineering company. Chapter 4 summarizes the ARUP studies, which exist as large online appendices to this PDDR.

This PDDR is a technical document, not a project execution plan. Accordingly, it does not address every aspect of the ERL project. A project of this magnitude has many on-going considerations that range beyond technical aspects, e.g., costs of construction and operation, discussions with state and local zoning boards, potential partners on the project, input from the scientific community about the best complement of beamlines, facility management models, detailed plans for how to transition from the presently operating CHESS facility to an ERL facility, etc. Although a great deal of attention has been given to such considerations, discussions about them are beyond the scope of this PDDR.

References

[1] W. Friedrich, P. K. and M. Laue. *Interferencz-Erscheinungen bei Roentgenstrahlen.* Sitzungberichte Bayer, pages 303–322 (1912).

[2] Laue, M. *Interferenczerscheinungen bei Roentgenstrahlen.* Sitzberichte Bayer, pages 363–373 (1912).

[3] Bragg, W. H. and W. L. Bragg. *The Structure of Diamond.* Proceedings of the Royal Society of London Serial A 89, pages 277–291 (1913).

[4] Bragg, W. L. *The Structure of Some Crystals as Indicated by their Diffraction of X-Rays.* Proceedings of the Royal Society of London Serial A 89, pages 248–277 (1913).

[5] Watson, J. D. and F. H. C. Crick. *A Structure for Deoxyribose Nucleaic Acid.* Nature 171, pages 737–738 (1953).

[6] Rossmann, M. G., *et al.* *Structure of a human common cold virus and functional relationship to other picornaviruses.* Nature 317, pages 145–153 (1985).

[7] Chapman, H. N., *et al.* *Femtosecond X-ray protein nanocrystallography.* Nature, **470** (7332), pages 73–77 (2011).

[8] Bilderback, D. H., *et al.* *Energy recovery linac (ERL) coherent hard X-ray sources.* New Journal of Physics 12 (3) (2010).

[9] Chao, A. W. and M. Tigner. *Handbook of Accelerator Physics and Engineering (3rd printing)* (2006).

[10] Wiedemann, H. *Particle Accelerator Physics I.* Springer Verlag, Berlin, second edition (1999).

[11] Balewski, K., *et al.* *Commissioning results of the beam diagnostics for the Petra III Light Sources.* In *Proceedings of DIPAC09, Basel, Switzerland* (2009).

[12] Kwang-Je Kim, Y. S. and S. Reiche. *A Proposal for an X-ray Free-Electron Laser Oscillator with an Energy-Recovery Linac* (2008).

[13] Feng, J., *et al.* *Structures and Potential Superconductivity in SiH_4 at High Pressure: En Route to "Metallic Hydrogen".* Phys. Rev. Lett., **96** (1), page 017006 (Jan 2006). doi:10.1103/PhysRevLett.96.017006.

[14] Grochala, W., *et al.* *The Chemical Imagination at Work in Very Tight Places.* Angewandte Chemie-International Edition, **46** (20), pages 3620–3642 (2007).

[15] Jayaraman, A. *Diamond anvil cell and high-pressure physical investigations.* Rev. Mod. Phys., **55** (1), page 65 (Jan 1983). doi:10.1103/RevModPhys.55.65.

[16] Vohra, Y., H. Luo, and A. Ruoff. *Optical-Properties of Diamond at Pressures of the Center of Earth.* Applied Physics Letters, **57** (10), pages 1007–1009 (1990).

[17] Held, G. A. and J. D. Brock. *Calculation of x-ray-diffraction profiles from vicinal surfaces*. Phys. Rev. B, **51** (11), pages 7262–7268 (Mar 1995). doi:10.1103/PhysRevB.51.7262.

[18] Kumar, K. S., H. V. Swygenhoven, and S. Suresh. *Mechanical behavior of nanocrystalline metals and alloys*. Acta Materialia, **51** (19), pages 5743 – 5774 (2003). ISSN 1359-6454. doi:DOI:10.1016/j.actamat.2003.08.032. The Golden Jubilee Issue. Selected topics in Materials Science and Engineering: Past, Present and Future.

[19] Cargill, G. S. I. *Microscopy: Extra dimension with X-rays*. Nature, **415**, pages 844–845 (February 2002). Doi:10.1038/415844a.

[20] Fu, X., *et al. Non-destructive mapping of grains in three dimensions*. Scripta Materialia, **49** (11), pages 1093–1096 (December 2003). Doi:10.1016/j.scriptamat.2003.08.007.

[21] Poulsen, H., *et al.* Materials Science Forum, **467-470**, pages 1363–1372 (2004).

[22] Ice, G. *KB Mirrors and Nanobeam Materials Science*. Presentation (June 2006). http://erl.chess.cornell.edu/gatherings/erl%20workshop/presentations/ws6/Icecondlock.pdf.

[23] Larson, B. C., *et al. Three-dimensional X-ray structural microscopy with submicrometre resolution*. Nature, **415**, pages 887–890 (February 2002). Doi:10.1038/415887a.

[24] Yang, W., *et al. Differential-aperture X-ray structural microscopy: a submicron-resolution three-dimensional probe of local microstructure and strain*. Micron, **35** (6), pages 431 – 439 (2004). ISSN 0968-4328. doi:DOI:10.1016/j.micron.2004.02.004. International Wuhan Symposium on Advanced Electron Microscopy.

[25] Williams, G. J., *et al. Three-Dimensional Imaging of Microstructure in Au Nanocrystals*. Phys. Rev. Lett., **90** (17), page 175501 (Apr 2003). doi:10.1103/PhysRevLett.90.175501.

[26] Pfeifer, M. A., *et al. Three-dimensional mapping of a deformation field inside a nanocrystal*. Nature, **442**, pages 63–66 (July 2006). Doi:10.1038/nature04867.

[27] Howells, M., *et al. An assessment of the resolution limitation due to radiation-damage in X-ray diffraction microscopy*. Journal of Electron Spectroscopy and Related Phenomena, **170** (1-3), pages 4 – 12 (2009). ISSN 0368-2048. doi:DOI:10.1016/j.elspec.2008.10.008. Radiation Damage.

[28] Zuo, J. M., *et al. Atomic Resolution Imaging of a Carbon Nanotube from Diffraction Intensities*. Science, **300** (5624), pages 1419–1421 (2003). doi:10.1126/science.1083887.

[29] Neutze, R., *et al. Potential for biomolecular imaging with femtosecond X-ray pulses*. Nature, **406**, pages 752–757 (August 2000). Doi:10.1038/35021099.

[30] Spence, J. C. H., *et al. Diffraction and imaging from a beam of laser-aligned proteins: resolution limits*. Acta Crystallographica Section A, **61** (2), pages 237–245 (Mar 2005). doi:10.1107/S0108767305002710.

[31] Starodub, D., *et al.* *Dose, exposure time and resolution in serial X-ray crystallography.* Journal of Synchrotron Radiation, **15** (1), pages 62–73 (Jan 2008). doi: 10.1107/S0909049507048893.

[32] Saldin, D. K., *et al.* *Structure of isolated biomolecules obtained from ultrashort x-ray pulses: exploiting the symmetry of random orientations.* Journal of Physics: Condensed Matter, **21** (13), page 134014 (2009).

[33] Anderson, P. *Viewpoint: The Future (letter).* Science, **267**, pages 1615–1616 (March 1995). DOI: 10.1126/science.267.5204.1615-e.

[34] Miao, J., *et al.* *Extending X-ray crystallography to allow the imaging of noncrystalline materials, cells, and single protein complexes.* Annual Review of Physical Chemistry, **59**, pages 387–410 (2008). ISSN 0066-426X. doi:{10.1146/annurev.physchem.59.032607.093642}.

[35] Rodenburg, J. M., *et al.* *Hard-X-Ray Lensless Imaging of Extended Objects.* Phys. Rev. Lett., **98** (3), page 034801 (Jan 2007). doi:10.1103/PhysRevLett.98.034801.

[36] Sutton, M. *Third Generation Hard X-ray Synchrotron Sources: Source Properties, Optics, and Experimental Techniques*, chapter Coherent X-ray Diffraction, pages 101–123. John Wiley & Sons: NY (2002).

[37] Wochner, P., *et al.* *X-ray cross correlation analysis uncovers hidden local symmetries in disordered matter.* Proceedings of the National Academy of Sciences, **106** (28), pages 11511–11514 (2009). doi:10.1073/pnas.0905337106.

[38] Park, H. Y., *et al.* *Achieving Uniform Mixing in a Microfluidic Device: Hydrodynamic Focusing Prior to Mixing.* Analytical Chemistry, **78** (13), pages 4465–4473 (2006). doi: 10.1021/ac060572n. PMID: 16808455.

[39] Pollack, L., *et al.* *Compactness of the Denatured State of a Fast-Folding Protein Measured by Submillisecond Small-Angle X-Ray Scattering.* Proceedings of the National Academy of Sciences of the United States of America, **96** (18), pages pp. 10115–10117 (1999). ISSN 00278424.

[40] Pollack, L., *et al.* *Time Resolved Collapse of a Folding Protein Observed with Small Angle X-Ray Scattering.* Phys. Rev. Lett., **86** (21), pages 4962–4965 (May 2001). doi: 10.1103/PhysRevLett.86.4962.

[41] Kwok, L. W., *et al.* *Concordant Exploration of the Kinetics of RNA Folding from Global and Local Perspectives.* Journal of Molecular Biology, **355** (2), pages 282 – 293 (2006). ISSN 0022-2836. doi:DOI:10.1016/j.jmb.2005.10.070.

[42] Russell, R., *et al.* *Rapid compaction during RNA folding.* Proceedings of the National Academy of Sciences of the United States of America, **99** (7), pages 4266–4271 (2002). doi:10.1073/pnas.072589599.

[43] Fenter, P., *et al.* *Observation of subnanometre-high surface topography with X-ray reflection phase-contrast microscopy*. Nature Physics, **2** (10), pages 700–704 (2006). Doi:10.1038/nphys419.

[44] Ferguson, J. D., *et al.* *Measurements of Surface Diffusivity and Coarsening during Pulsed Laser Deposition*. Phys. Rev. Lett., **103** (25), page 256103 (Dec 2009). doi:10.1103/PhysRevLett.103.256103.

[45] Shpyrko, G., *et al.* *Direct measurement of antiferromagnetic domain fluctuations*. Nature, **447** (7140), pages 68–71 (May 2007). Doi:10.1038/nature05776.

[46] Goodenough, J. *et al.* *Basic research needs for electrical energy storage*. Report, United States Department of Energy (July 2007). http://www.sc.doe.gov/bes/reports/files/EES_rpt.pdf.

[47] Grätzel, M. *Dye-sensitized solar cells*. Journal of Photochemistry and Photobiology C: Photochemistry Reviews, **4** (2), pages 145 – 153 (2003). ISSN 1389-5567. doi:10.1016/S1389-5567(03)00026-1.

[48] Grätzel, M. *Applied physics: Solar cells to dye for*. Nature, **6923** (421), pages 586–587 (February 2003). Doi:10.1038/421586a.

[49] Tigner, M. *A Possible Apparatus for Electron Clashing-Beam Experiments*. Nuovo Cimento, 37 (3), pages 1221–1228 (1965).

[50] Neil, G. R., *et al.* *Sustained Kilowatt lasing in a free-electron laser with same-cell energy recovery*. Phys. Rev. Lett, pages 662–665 (2000).

[51] Smith, T. I., *et al.* *Development of the SCA/FEL for use in biomedical and materials science experiments*. Nucl. Instr. and Meth. A, pages 1–7 (1987).

[52] Bilderback, D., *et al.* *New Energy Recovery Linac Source of Synchrotron X-Rays*. Synchotron Radiation News, 14 (3), pages 12–21 (2001).

[53] Gruner, S. M., *et al.* *Study for a proposed Phase I Energy Recovery Linac (ERL) Synchrotron Light Source at Cornell University*. Technical report (2001).

[54] Hoffstaetter, G., *et al.* *Progress toward an ERL Extension to CESR*. Technical report (2007).

[55] Hoffstaetter, G. *et al.* *Challenges for Beams in an ERL Extension to CESR*. In *Proceedings of EPAC08* (2008).

[56] *3rd international ERL workshop* (2009). www.lepp.cornell.edu/Events/ERL09.

[57] C. Riekel, M. B. and G. Schertler. *Protein crystallography microdiffraction*. Current Opinion in Structural Biology, vol. 15, pages 556–562 (2005).

[58] Riekel, C. and R. Davies. *Applications of synchrotron radiation micro-focus techniques to the study of polymer and biopolymer fibers*. Current Opinion in Colloid & Interface Science, vol. 9, pages 396–403 (2005).

[59] Roth, S., *et al.* *Self-assembled gradient nanoparticle-polymer multilayers investigated by an advanced characterization method: microbeam grazing incidence X-ray scattering.* Applied Physics Letters, 82, pages 1935–1937 (2003).

[60] Riekel, C. *New avenues in X-ray microbeam experiments.* Reports on Progress in Physics, pages 233–262 (2000).

[61] Riekel, C., M. Burghammer, and M. Muller. *Microbeam small-angle scattering experiments and their combination with microdiffraction.* Journal of Applied Crystallography, vol. 33, pages 421–423 (2000).

[62] Rindby, A. *Progress in X-ray Microbeam Spectroscopy.* X-Ray Spectrometry, vol. 22, pages 187–191 (1993).

[63] B.C.Larson, *et al.* *Three-dimensional X-ray structural microscopy with submicrometre resolution.* Nature, vol. 45, pages 887–890 (2002).

[64] Bilderback, D. H. and R. Huang. *Are Atom-sized X-Ray Experiments Possible?* In T. Warwick *et al.*, editors, *AIP Conference Proceedings*, volume 705, pages 1271–1273 (2004).

[65] ARUP. *Energy Recovery Project Definition Design, Volume I Report.* Technical report (2010).

[66] ARUP. *Energy Recovery Linac Project Definition Design, Volume II Drawings.* Technical report (2010).

[67] UTAP. *Energy Recovery LINAC Project Definition Design, Volume I Report.* Technical report (2010).

[68] ARUP. *Project Definition Design Study for the ERL upgrade to CESR, Volume 1-Technical Report.* Technical report (2008).

[69] Zaicenco, A. Technical report, Terrascience Systems Ltd. (2010).

[70] *Budgetary Estimate for ERL Beamline Components Report 30086-BP-8384-0.* Technical report, Research Instruments (2010). Report is on file at Cornell.

[71] *Helium Refrigeration System for the ERL Cornell Project, Technical Proposal ALCS-2010-TP-008.* Technical report, Air Liquide Cryogenic Services (2010). Report is on file at Cornell.

[72] *Cryogenic Plant Study and Budgetary Estimate for ERL Facility, Proposal, November 2006.* Proposal submitted to CLASSE by Linde Kryotechnik, AG. Report is on file at Cornell.

[73] ARUP. *Energy Recovery Linac Project Definition Design, Volume III - Cost plan and schedule.* Technical report (2010).

[74] Narayanamurti, V. *NSF Future Light Sources Report.* Technical report (2008).

[75] Gruner, S. *Phase 1 Energy Recovery Linac (ERL) Synchrotron Light Source at Cornell University* (2005). NSF grant PHY-0131598.

[76] Gruner, S. *Energy Recovery Linac (ERL) R&D 2-1-09 to 3-31-10* (2009). NSF grant DMR-0937466.

[77] Gruner, S. *IMR: Phase 1B Energy Recovery Linac (ERL) Technology R&D* (2010). NSF proposal DMR-0807731.

[78] Hartman, P. and D. H. Tomboulian. *Ultraviolet Radiation from the Cornell Synchrotron*. Phys. Rev., **87**, page 233 (1952). In Minutes of the 1952 Washington Meeting.

[79] Hartman, P. L. and D. H. Tomboulian. *Far Ultraviolet Radiation from the Cornell Synchrotron*. Phys. Rev., **91** (6), pages 1577–1578 (Sep 1953). doi:10.1103/PhysRev.91.1577.

[80] Tomboulian, D. H. and P. L. Hartman. *Spectral Distribution Curves of the Far Ultraviolet Radiation from the Cornell Synchrotron*. Physical Review, vol. 95 (1954).

[81] Tomboulian, D. H. and P. L. Hartman. *Spectral and Angular Distribution of Ultraviolet Radiation from the 300-Mev Cornell Synchrotron*. Phys. Rev., **102** (6), pages 1423–1447 (Jun 1956). doi:10.1103/PhysRev.102.1423.

[82] Batterman, B. W. and N. W. Ashcroft. *Chess - New Synchrotron Radiation Facility at Cornell*. Science, vol. 206, pages 157–161 (1979).

[83] *Cornell ERL Workshops* (2006). http://erl.chess.cornell.edu/gatherings/erl%20workshop/index.htm.

[84] *XDL 2011 Workshops: Science at the hard X-ray Diffraction Limit* (2011). http://erl.chess.cornell.edu/gatherings/2011_Workshops/index.htm.